YAP1 Activation by Human Papillomavirus E7 Promotes Basal Cell Identity in Squamous Epithelia

Joshua Hatterschide[1], Paola Castagnino[1], Hee Won Kim[1], Steven M. Sperry[2], Kathleen T. Montone[3], Devraj Basu[1], Elizabeth A. White[1*]

[1]Department of Otorhinolaryngology: Head and Neck Surgery, University of Pennsylvania Perelman School of Medicine, Philadelphia, PA, USA

[2]Current address: Department of Otolaryngology-Head and Neck Surgery, Aurora St. Luke's Medical Center, Milwaukee, Wisconsin, U.S.A.

[3]Department of Pathology and Laboratory Medicine, University of Pennsylvania Perelman School of Medicine, Philadelphia, PA, USA

* Correspondence: Elizabeth A. White, eawhite@pennmedicine.upenn.edu

Abstract

Persistent human papillomavirus (HPV) infection of stratified squamous epithelial cells causes nearly five percent of cancer cases worldwide. HPV-positive oropharyngeal cancers harbor few mutations in the Hippo signaling pathway compared to HPV-negative cancers at the same anatomical site, prompting the hypothesis that an HPV-encoded protein inactivates the Hippo pathway and activates the Hippo effector YAP1. The HPV E7 oncoprotein is required for HPV infection and for HPV-mediated oncogenic transformation. We investigated the effects of HPV oncoproteins on YAP1 and found that E7 activates YAP1, promoting YAP1 nuclear localization in basal epithelial cells. YAP1 activation by HPV E7 required that E7 bind and degrade the tumor suppressor PTPN14. E7 required YAP1 transcriptional activity to extend the lifespan of primary keratinocytes, indicating that YAP1 activation contributes to E7 carcinogenic activity. Maintaining infection in basal cells is critical for HPV persistence, and here we demonstrate that YAP1 activation causes HPV E7 expressing cells to be retained in the basal compartment of stratified epithelia. We propose that YAP1 activation resulting from PTPN14 inactivation is an essential, targetable activity of the HPV E7 oncoprotein relevant to HPV infection and carcinogenesis.

Introduction

Human papillomaviruses (HPV) are non-enveloped viruses with circular double-stranded DNA genomes that infect keratinocytes in stratified squamous epithelia (Doorbar et al., 2015; Graham, 2017; McBride, 2017). Although most HPV infections are cleared by the immune system, some infections persist and form higher grade lesions that can lead to cancer (Koshiol et al., 2008; McBride, 2021; Radley et al., 2016; Rositch et al., 2013). HPV infection at mucosal epithelial sites causes cancers including oropharyngeal, cervical, vaginal, penile, and anal malignancies (de Martel et al., 2017; Gillison et al., 2015). Nearly 5% of human cancer cases are caused by persistent infection with one of the high-risk (oncogenic) human papillomavirus genotypes (de Martel et al., 2020).

Inactivation of host cell tumor suppressors by the high-risk HPV E6 and E7 oncoproteins modulates cellular processes that enable HPV persistence. Two well-characterized instances of tumor suppressor inactivation by HPV are high-risk HPV E6 proteins targeting p53 for proteasome-mediated degradation and high-risk HPV E7 proteins binding and degrading the retinoblastoma protein (RB1) (Heck et al., 1992; Münger et al., 1989; Scheffner et al., 1990; Seavey et al., 1999; Werness et al., 1990). Both p53 degradation and RB1 inactivation are required for productive HPV infection (Collins et al., 2005; Flores et al., 2000; Kho et al., 2013; McLaughlin-Drubin et al., 2005; Wang et al., 2009). In addition to supporting productive infection, E7 is essential for HPV-mediated carcinogenesis (Mirabello et al., 2017). The impact of the HPV oncoproteins on cell growth control pathways is reflected in human cancer genomic data: genes in the p53 pathway and in the RB1-related cell cycle pathway are frequently mutated in HPV-negative head and neck squamous cell carcinoma (HNSCC) but infrequently mutated in HPV-positive HNSCC (Sanchez-Vega et al., 2018).

Although some of the growth-promoting activities of high-risk HPV E6 and E7 are well established, open questions remain. RB1 binding/degradation by high-risk HPV E7 is necessary but insufficient for E7 transforming activity (Balsitis et al., 2006, 2005; Banks et al., 1990; Ciccolini

et al., 1994; Helt and Galloway, 2002; Huh et al., 2005; Ibaraki et al., 1993; Jewers et al., 1992; Phelps et al., 1992; Strati and Lambert, 2007; White et al., 2015). Papillomavirus researchers have sought to identify one or more activities of HPV E7 that cooperate with RB1 inactivation to promote carcinogenesis and to identify the cellular pathway affected by such an activity. Human cancer genomic data indicates that like the p53 and cell cycle pathways, the Hippo signaling pathway is more frequently mutated in HPV-negative than in HPV-positive HNSCC. The core Hippo pathway consists of a kinase cascade upstream of the effector proteins Yes-Associated Protein (YAP1) and its paralogue TAZ. When the Hippo kinases are inactive, YAP1 and TAZ are activated and translocate to the nucleus. In stratified squamous epithelia YAP1 is primarily expressed in the basal layer, where YAP1 activation is regulated by contextual cues including cell density, tension in the extracellular matrix, and contact with the basement membrane (Elbediwy et al., 2016; Totaro et al., 2017; Zhang et al., 2011). In normal stratified squamous epithelia, activation of YAP1 and TAZ promotes expansion of the basal cell compartment, and inhibition of YAP1 and TAZ allows keratinocytes to differentiate (Beverdam et al., 2013; Elbediwy and Thompson, 2018; Schlegelmilch et al., 2011; Totaro et al., 2017; Yuan et al., 2020; Zhang et al., 2011). Mutations in many of the tumor suppressors upstream of YAP1/TAZ are common in a variety of cancer types (Moroishi et al., 2015).

Non-receptor protein tyrosine phosphatase 14 (PTPN14) has been implicated as a tumor suppressor and negative regulator of YAP1 (Knight et al., 2018; Mello et al., 2017; Poernbacher et al., 2012; Wang et al., 2012). Diverse HPV E7 bind directly to PTPN14 and recruit the E3 ligase UBR4 to direct PTPN14 for proteasome-mediated degradation (Szalmás et al., 2017; White et al., 2016, 2012b; Yun et al., 2019). We have shown that PTPN14 degradation and RB1 binding/degradation are separable activities of HPV E7 that each contribute to E7 carcinogenic activity (Hatterschide et al., 2020, 2019; White et al., 2016). However, the downstream consequences of PTPN14 degradation are poorly understood, and so far we have not observed

that PTPN14 inactivation in human keratinocytes causes an increase in canonical YAP1 target genes *CTGF* and *CYR61*.

These observations regarding an additional transforming activity of HPV E7, the ability of E7 to inactivate PTPN14, and the relative paucity of mutations in the Hippo pathway in HPV-positive HNSCC led us to hypothesize that HPV E7-mediated activation of YAP1 is required for the transforming activity of high-risk HPV E7. Here we show that expression of high-risk HPV E7 is sufficient to activate YAP1 and that HPV E7 requires YAP1/TAZ-TEAD transcriptional activity to promote cell growth. We demonstrate that HPV E7 must bind PTPN14 to activate YAP1 and that PTPN14 inactivation alone is sufficient to activate YAP1. YAP1 activation by HPV E7 is restricted to the basal layer of the epithelium where we found *PTPN14* expression to be enriched.

Our finding that either HPV E7 or PTPN14 loss activate YAP1 specifically in basal epithelial cells led us to investigate the role of YAP1 activation during normal HPV infection. HPV infection begins in basal epithelial keratinocytes (Day and Schelhaas, 2014; Pyeon et al., 2009; Roberts et al., 2007) and infected basal cells are the site of persistent HPV infection. The basal cell compartment contains the only long-lived cells in the epithelium and the HPV genome can be maintained in dividing basal cells without productive replication (Egawa et al., 2012; Parish et al., 2006; You et al., 2004). Activation of YAP1 and TAZ has been proposed to maintain the progenitor cell state in several different epithelia (Beverdam et al., 2013; Heng et al., 2020; Hicks-Berthet et al., 2021; Szymaniak et al., 2015; Yimlamai et al., 2014; Zhao et al., 2014). If YAP1 activation by E7 promotes the maintenance of a basal cell state in stratified squamous epithelia, YAP1 activation could facilitate the persistence of HPV-positive cells. Testing this hypothesis, we found that YAP1 activation and PTPN14 degradation by E7 both promote the maintenance of cells in the basal compartment of stratified epithelia. We propose that YAP1 activation facilitates HPV persistence and contributes to the carcinogenic activity of high-risk HPV E7.

Results

HPV E7 activates YAP1 in basal keratinocytes

A comprehensive analysis of somatic mutations and copy number variations in human tumor samples revealed that the cell cycle, p53, and Hippo pathways are the three pathways that exhibit the greatest difference in alteration frequency in HPV-negative vs HPV-positive HNSCC (Sanchez-Vega et al., 2018). We used data made available by The Cancer Genome Atlas (TCGA) through cBioPortal (Lawrence et al., 2015) to recapitulate the finding that genes in these pathways are altered at a lower frequency in HPV-positive than in HPV-negative HNSCC (Figure 1A and Figure 1—figure supplement 1). However, most HPV-positive HNSCC arise in the oropharynx. We repeated the analysis of pathway alteration rates using data only from HPV-positive and HPV-negative oropharyngeal squamous cell carcinomas (OPSCC) (Figure 1A and Figure 1—figure supplement 1). Consistent with previous findings, HPV-negative OPSCC were more frequently altered in the p53, cell cycle, and Hippo pathways than HPV-positive OPSCC. Many of the Hippo pathway alterations in HPV-negative HNSCC or OPSCC are amplification of the YAP1/TAZ oncogenes or inactivating mutation in an upstream inhibitor of YAP1/TAZ. Either alteration type is consistent with a carcinogenic role for YAP1 activation in HNSCC.

To test whether an HPV-encoded protein activates YAP1, we grew three dimensional (3D) organotypic epithelial cultures to model the differentiation of keratinocytes into basal and suprabasal compartments. Organotypic cultures of primary human foreskin keratinocytes (HFK) harboring an HPV18 genome exhibited increased YAP1 staining and increased YAP1 nuclear localization, indicative of YAP1 activation, particularly in the basal layer of the epithelium, compared to HFK cultures (Figure 1B and Figure 1—figure supplement 2A,B). Proliferating cell nuclear antigen (PCNA) transcription increases upon RB1 inactivation and is a marker of HPV E7 expression. In contrast to the basal layer-specific compartmentalization of YAP1 activation in the HPV18 genome containing cells, PCNA levels were increased in these cultures in both the basal and suprabasal layers of the epithelium.

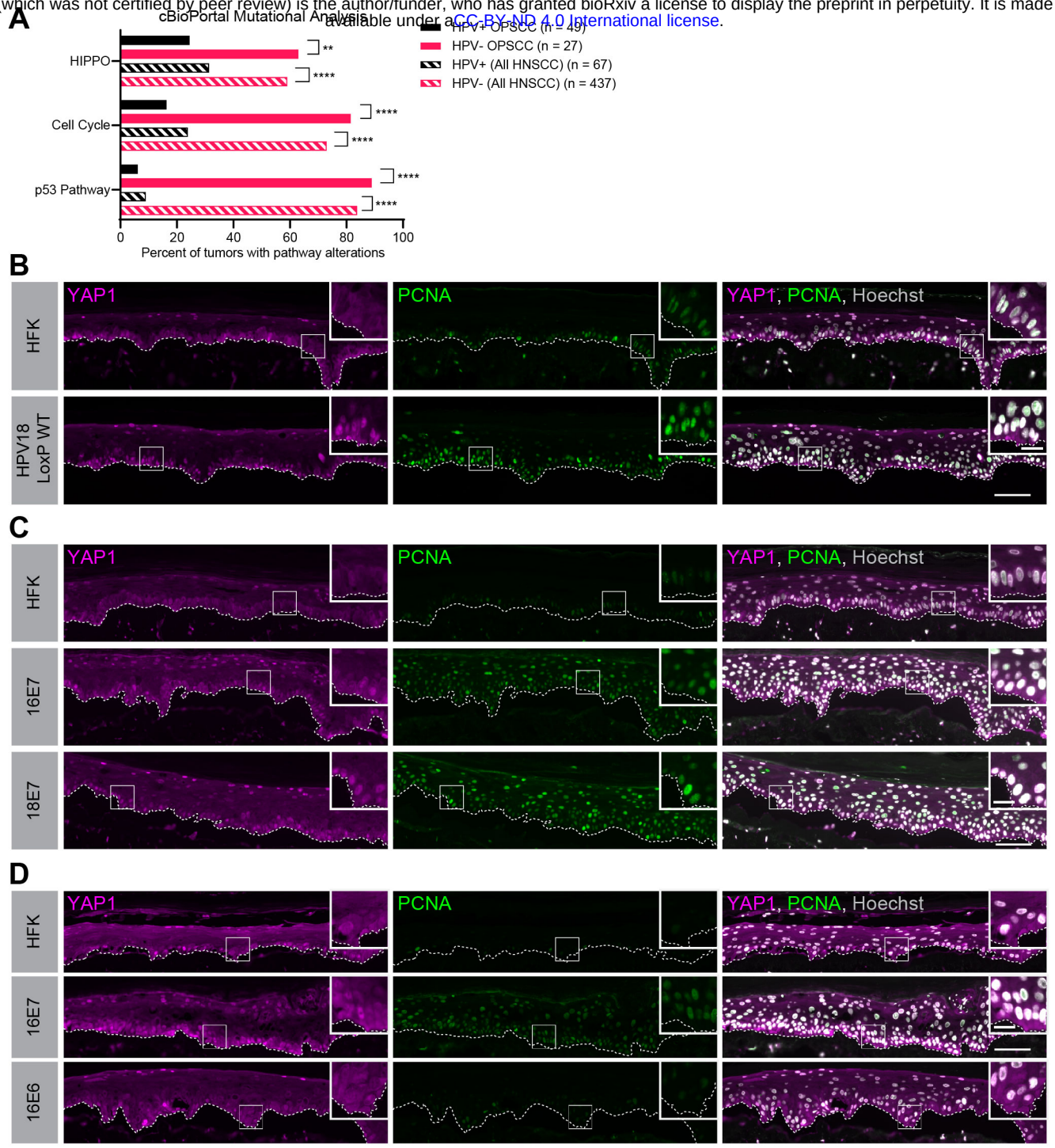

Figure 1 | HPV E7 activates YAP1 in basal epithelial keratinocytes. (A) cBioPortal analysis for total genomic mutations and copy number alterations in HPV+/- OPSCC and HNSCC. Graph displays the percent of tumors with alterations in each pathway. Statistical significance was determined by Fisher's exact test. (B-D) Organotypic cultures were grown from primary HFK, HFK harboring the HPV18 genome, or HFK transduced with retroviral expression encoding HPV E6 or E7 proteins. FFPE sections of cultures grown from (C) HFK or HFK harboring the HPV18 genome, (D) HFK or HFK expressing HPV16 E7 or HPV18 E7, or (E) HFK or HFK expressing HPV16 E6 or HPV16 E7 were stained for YAP1 (magenta), PCNA (green), and Hoechst (gray). White dashed lines indicate the basement membrane. White boxes indicate the location of insets in main images. Main image scale bars = 100 μm. Inset scale bars = 25 μm.

We next tested whether high-risk HPV E6 or E7 alone was sufficient to activate YAP1. HFK transduced with retroviral expression vectors encoding HPV16 E6, HPV16 E7, or HPV18 E7 were used to grow organotypic cultures. YAP1 expression and nuclear localization were increased in the HPV16 E7 and HPV18 E7 expressing cells relative to parental HFK cells (Figure 1C and Figure 1—figure supplement 3A-C). As in the HPV18 genome-containing cells, YAP1 activation was restricted to the basal epithelial layer. YAP1 expression or nuclear localization did not increase in organotypic cultures of HPV16 E6 expressing cells (Figure 1D and Figure 1—figure supplement 4). Constitutive expression of either HPV16 E7 or HPV18 E7 induced PCNA expression in basal and suprabasal cells. We conclude that HPV promotes increased YAP1 expression and nuclear localization in basal keratinocytes and that E7 is sufficient for YAP1 activation.

HPV E7 activates YAP1 in keratinocytes through PTPN14 degradation

We previously discovered that HPV E7 targets the YAP1 inhibitor PTPN14 for proteasome-mediated degradation (White et al., 2016, 2012b). We tested whether loss of PTPN14 expression in keratinocytes was sufficient to activate YAP1 in stratified epithelia by growing 3D organotypic cultures from previously described control and PTPN14 knockout (KO) N/Tert-Cas9 keratinocytes (Hatterschide et al., 2019). We found that YAP1 levels and YAP1 nuclear localization were increased in PTPN14 KO cultures compared to controls (Figure 2A and Figure 2—figure supplement 1A-C). YAP1 activation in basal epithelial cells lacking PTPN14 was comparable to YAP1 activation in HPV E7 cells. We conclude that loss of PTPN14 expression activates YAP1 in basal keratinocytes.

A highly conserved C-terminal arginine in E7 makes a direct interaction with the C-terminus of PTPN14, and the HPV18 E7 R84S variant is unable to bind or degrade PTPN14 (Hatterschide et al., 2020; Yun et al., 2019). To test whether PTPN14 degradation by HPV E7 is required for activation of YAP1, we grew 3D organotypic cultures using primary HFK transduced

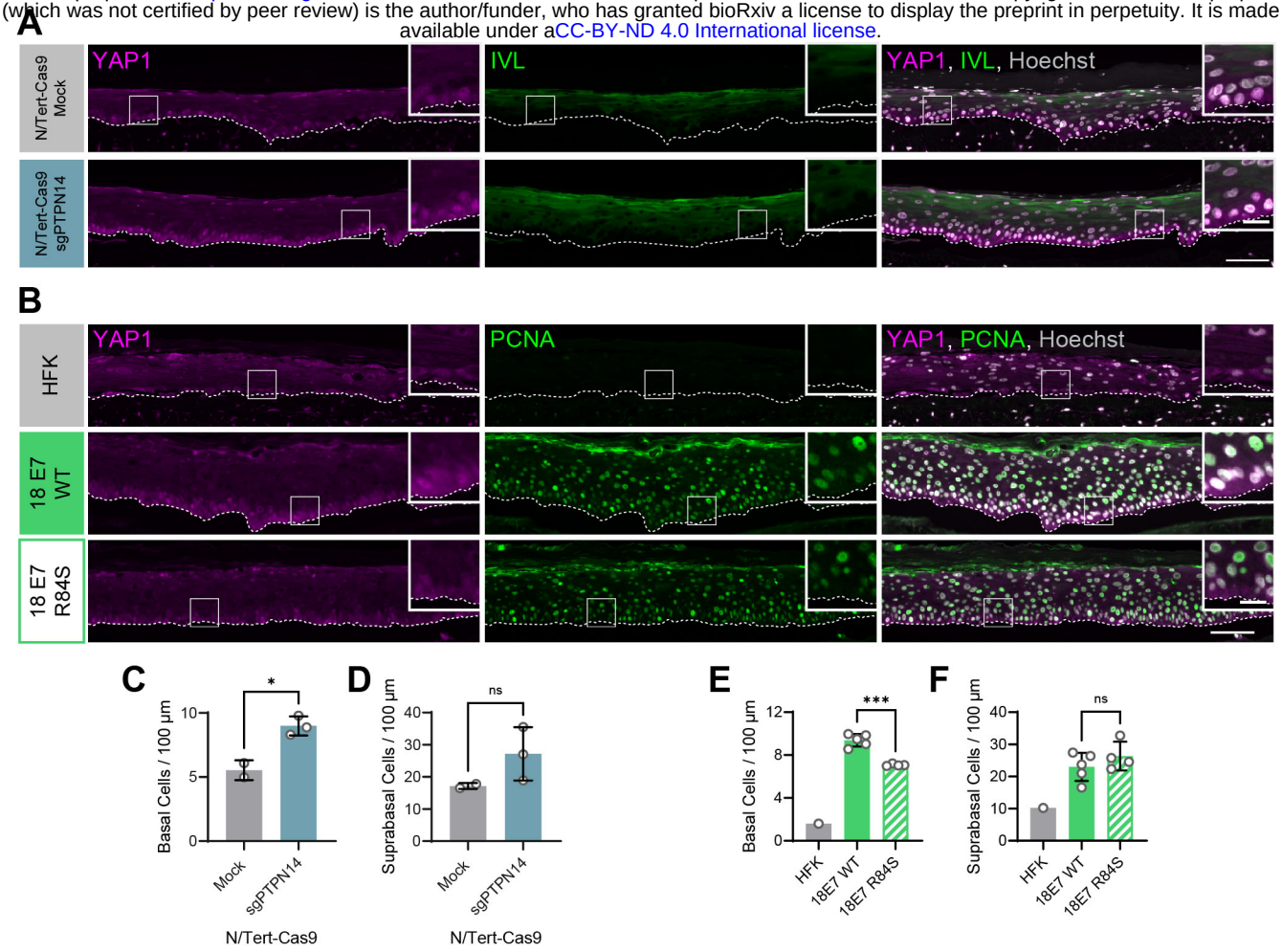

Figure 2 | HPV E7 activates YAP1 in basal keratinocytes through PTPN14 degradation. Organotypic cultures were grown from N/Tert-Cas9 keratinocytes or primary HFK transduced with retroviral expression vectors encoding HPV18 E7 WT or R84S. (A) FFPE sections of cultures grown from mock or sgPTPN14 transfected N/Tert-Cas9 keratinocytes were stained for YAP1 (magenta), IVL (green), and Hoechst (Gray). (B) FFPE sections of cultures grown from parental HFK, HPV18 E7 WT or HPV18 E7 R84S expressing HFK were stained for YAP1 (magenta), PCNA (green), and Hoechst (Gray). White dashed lines indicate the basement membrane. White boxes indicate the location of insets in main images. Main image scale bars = 100 µm. Inset scale bars = 25 µm. (C-F) Quantification of the number of (C and E) basal cells and (D and F) suprabasal cells per 100 µm of epidermis. Graphs display the mean ± SD and each individual data point (independent cultures). Statistical significance was determined by ANOVA (*p<0.05, ***p<0.001).

with retroviral expression vectors encoding HPV18 E7 wild type (WT) or HPV18 E7 R84S. Indeed, YAP1 expression and nuclear localization in the basal layer of HPV18 E7 R84S cultures were reduced compared to HPV18 E7 WT controls (Figure 2B and Figure 2—figure supplement 2).

In addition to activating YAP1, PTPN14 loss increased basal cell density from an average of 5.5 cells per 100 μm in control cultures to 9.0 cells per 100 μm in PTPN14 KO cultures (Figure 2C). Basal cell density was higher in HPV18 E7 WT cultures (9.4 cells per 100 μm) than in HPV18 E7 R84S cultures (to 7.1 cells per 100 μm) (Figure 2E). No statistically significant difference in suprabasal cell density was observed in either comparison (Figure 2D,F). We conclude that E7 expression or PTPN14 loss in stratified squamous epithelia is sufficient to activate YAP1 in the basal layer of the epithelium and increase basal cell density.

PTPN14 expression is enriched in basal keratinocytes

YAP1 activation was restricted to basal epithelial cells in our organotypic cultures leading us to hypothesize that PTPN14 may act as a basal layer specific inhibitor of YAP1. We therefore sought to determine whether *PTPN14* expression is restricted to a specific subset of cells in the stratified epithelium. In a recent single cell-RNA seq analysis of human neonatal foreskin epidermis, *PTPN14* mRNA expression was enriched in the basal-III cluster, a subset of basal cells predicted to differentiate directly into spinous cells (Figure 3A,B) (S. Wang et al., 2020). *PTPN14* expression was higher in basal-III cells than in the spinous or granular cell clusters. To test whether *PTPN14* expression is higher in basal or suprabasal cells in our cultures, we used laser capture microdissection to isolate basal and suprabasal layers from 3D organotypic cultures grown from unmodified primary HFK (Figure 3C). We found that there was a ~5-fold enrichment of *PTPN14* mRNA in the basal epithelial layer compared to the suprabasal layers (Figure 3D). As expected, the basal integrins *ITGA6* and *ITGB4* were expressed in the basal layer (Figure 3E) and the differentiation markers *KRT1* and *IVL* were expressed in the suprabasal layers (Figure 3F). The same pattern of *PTPN14* mRNA expression was observed in an organotypic culture grown from

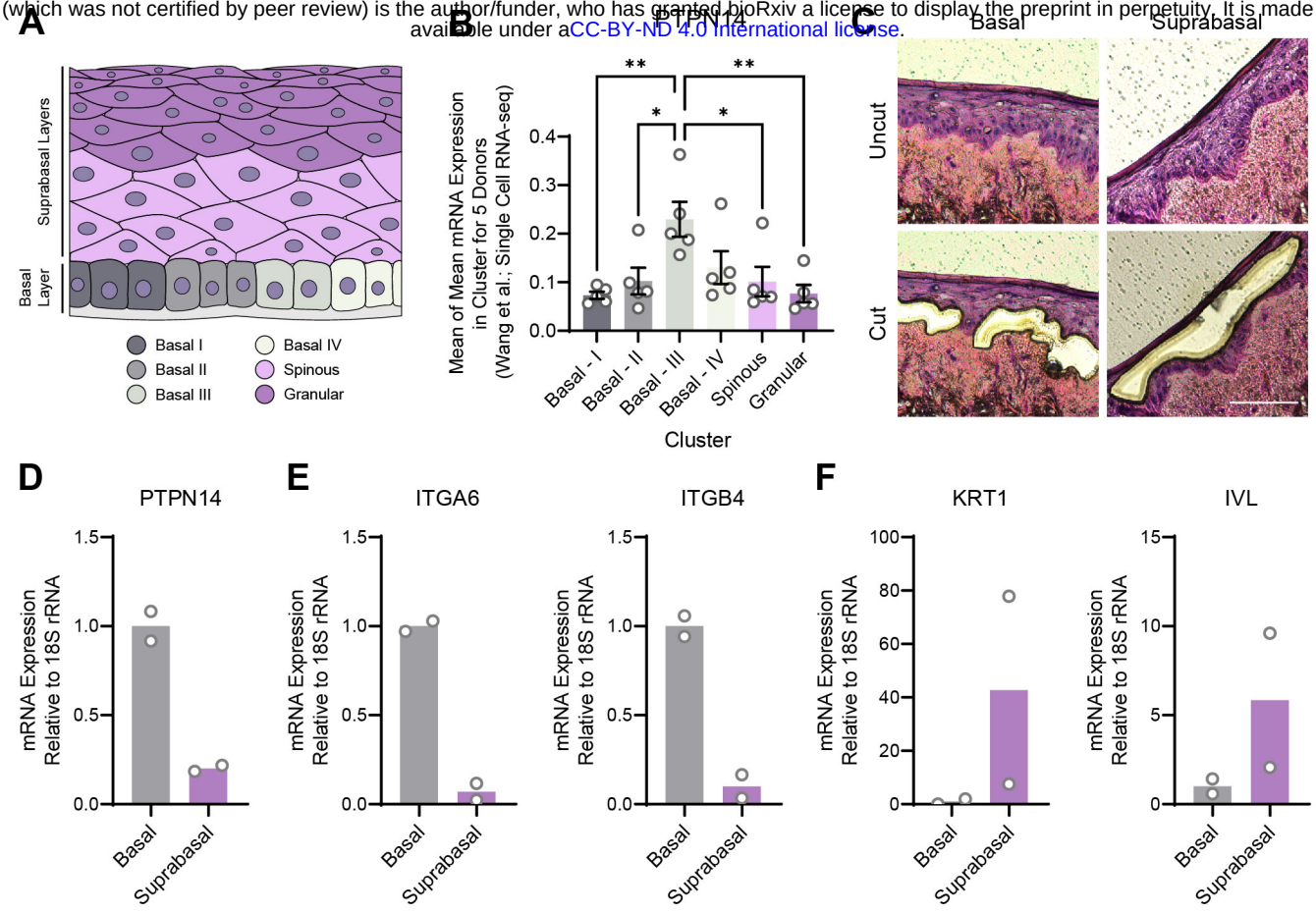

Figure 3 | PTPN14 expression is enriched in basal keratinocytes. (A-B) Single-cell RNA sequencing data and clustering analysis from Wang et al. was reanalyzed to assess PTPN14 expression in different subsets of epidermal cells. (A) Diagram of epidermis; shading depicts tissue localization of cell clusters. (B) For each donor, the mean of PTPN14 mRNA expression was calculated for each cell cluster. Graphs display the mean of PTPN14 mRNA expression for each donor (circles) as well as the mean of all five donors ± SEM (bars and error bars). Statistical significance was determined by ANOVA (*p<0.05, **p<0.01). (C-F) Basal and suprabasal layers from organotypic cultures were dissected using laser capture microdissection. (C) Representative images of HFK cultures before and after individual laser dissections. Hundreds of such cuts were performed per sample. (D-F) RNA was purified from isolated layers and qRT-PCR was used to assess the expression of PTPN14 (D), basal cell markers ITGA6 and ITGB4 (E), and differentiation markers KRT1 and IVL (F). Graphs display the mean and each individual data point.

primary HFK expressing HPV18 E7 WT (Figure 3—figure supplement 1A-C). We conclude that *PTPN14* mRNA is enriched in basal keratinocytes in the presence or absence of HPV E7. Our data support that PTPN14 acts as a YAP1 inhibitor specifically in the basal compartment of stratified epithelia.

YAP1/TAZ regulate differentiation downstream of PTPN14

In previous unbiased experiments we found that the primary effect of PTPN14 inactivation on transcription is to repress epithelial differentiation gene expression (Hatterschide et al., 2020, 2019). However, we also observed that PTPN14 inactivation did not increase expression of the canonical YAP1/TAZ targets *CTGF* and *CYR61*. Consistent with this difference there was minimal overlap between PTPN14-dependent differentially expressed genes and the genes listed in the MSigDB conserved YAP1 signature (Figure 4A). We therefore asked whether the ability of PTPN14 to regulate differentiation gene expression requires YAP1/TAZ as intermediates. Transduction of keratinocytes with a PTPN14 lentivirus induced the expression of the differentiation markers *KRT10* and *IVL* in a dose-dependent manner (Figure 4—figure supplement 1A-C). To test whether PTPN14 required YAP1/TAZ to increase *KRT1* and *IVL*, we transfected HFK with siRNAs targeting *YAP1* and *WWTR1* then transduced the cells with PTPN14 lentivirus (Figure 4B). HFK transfected with control siRNA exhibited the expected increase in *KRT1* and *IVL* after transduction with PTPN14 lentivirus (Figure 4C,D and Figure 4—figure supplement 2A,B). However, keratinocytes depleted of YAP1/TAZ did not express relatively more *KRT1* or *IVL* when PTPN14 was overexpressed than when it was not. We conclude that PTPN14 requires YAP1 and/or TAZ to regulate differentiation gene expression in keratinocytes. Both pairs of YAP1/TAZ siRNA had the same effect on differentiation in response to PTPN14 overexpression yet only one pair efficiently depleted TAZ protein levels (Figure 4B), leading us to speculate that YAP1 is the key intermediate connecting PTPN14 levels to differentiation gene expression.

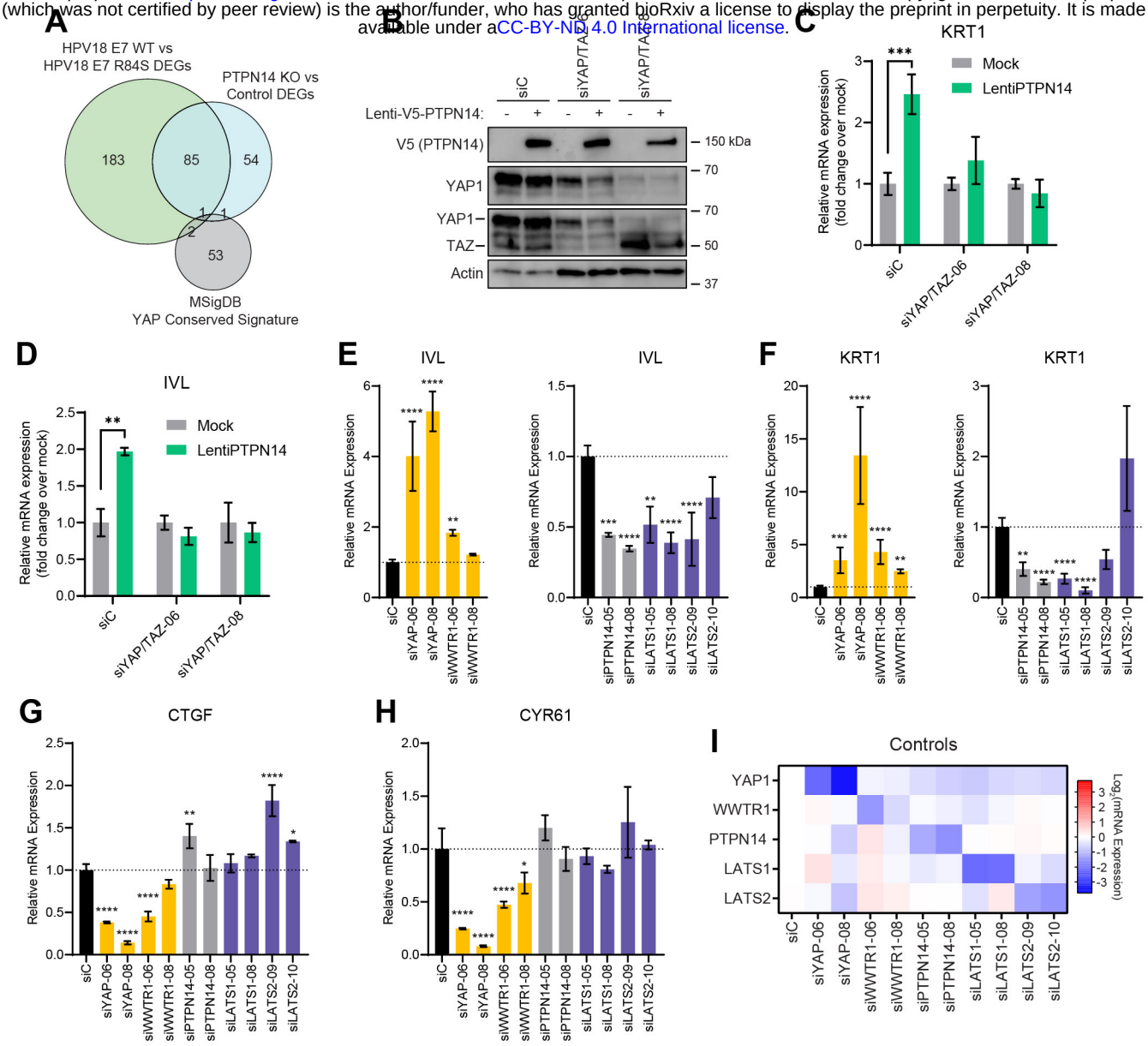

Figure 4 | YAP1/TAZ regulate differentiation downstream of PTPN14. (A) Venn diagram comparing the MSigDB YAP conserved signature to the differentially expressed genes (DEG) from our two published experiments that reflect PTPN14 loss in keratinocytes. (B-D) YAP1 and WWTR1 were simultaneously knocked down by siRNA transfection in HFK. Transfected HFK were then transduced with PTPN14 lentivirus at 24h post transfection. Cells were lysed for protein and total cellular RNA at 72h post transfection. (B) Cell lysates were subjected to SDS/PAGE/Western analysis and probed with antibodies to PTPN14, YAP1, TAZ, and Actin. (C and D) qRT-PCR was used to measure the expression of the differentiation markers KRT1 and IVL relative to G6PD. Graphs display fold change in gene expression relative to the mock transduced cells. (E-I) Primary HFK were transfected with siRNAs targeting YAP1, WWTR1 (TAZ), PTPN14, LATS1, and LATS2. Two siRNAs were used per target. qRT-PCR was used to measure gene expression for: the differentiation markers IVL (E) and KRT1 (F), and the canonical YAP1/TAZ targets CTGF (G) and CYR61 (H). Data confirming that individual siRNA transfections depleted intended transcripts is summarized in a heatmap of log2(fold-change) levels (I). Bar graphs display the mean ± SD of three independent replicates. Statistical significance was determined by ANOVA (*p<0.05, **p<0.01, ***p<0.001, ****p<0.0001).

Next, we tested whether repression of keratinocyte differentiation occurs upon loss of LATS1 and LATS2, the core Hippo pathway kinases that phosphorylate and inhibit YAP1 and TAZ. We used siRNAs to deplete *PTPN14*, *LATS1*, or *LATS2* and measured the expression of the differentiation markers *KRT1* and *IVL* (Figure 4E,F). Depletion of *PTPN14, LATS1,* or *LATS2* all decreased differentiation gene expression to a similar degree. Consistent with our previous experiments, none of the three knockdowns significantly affected the levels of *CTGF* or *CYR61* (Figure 4G-H). Direct depletion of *YAP1* or *WWTR1* affected both differentiation gene expression and *CTGF/CYR61* levels. *YAP1* knockdown always had a stronger effect than did *WWTR1* knockdown and our qRT-PCR analyses supported that *WWTR1* transcript levels were low in HFK. This result shows that inactivation of three different YAP1 inhibitors dampens differentiation gene expression and does not increase canonical YAP1 target gene expression in keratinocytes. Taken together, these data support that PTPN14 promotes differentiation through inhibition of YAP1/TAZ despite not affecting canonical YAP1/TAZ target genes.

HPV-positive HNSCC are less differentiated than HPV-negative HNSCC

We next asked whether the gene expression pattern observed downstream of PTPN14 loss is reflected in HPV-positive cancers. HPV-positive HNSCC have a strong propensity toward poorly differentiated, basaloid histology (Mendelsohn et al., 2010; Pai and Westra, 2009), which is reflected in their transcriptional profile (Hatterschide et al., 2019). We confirmed the relationship between HPV positivity and greater impairment of differentiation by immunohistochemical analysis of the differentiation marker KRT1 in sections of 14 HPV-negative tumors and 48 HPV-positive tumors (Figure 5A). 43% of HPV-negative tumors and 12.5% of HPV-positive tumors stained positive for KRT1. We additionally measured gene expression in patient-derived xenograft (PDX) models generated from human HNSCC. We measured *KRT1*, *KRT10*, and *IVL* levels using RNA extracted from 11 HPV-negative and 8 HPV-positive HNSCC PDX. Each differentiation marker was expressed at a markedly lower level in HPV-positive PDX than in HPV-negative PDX

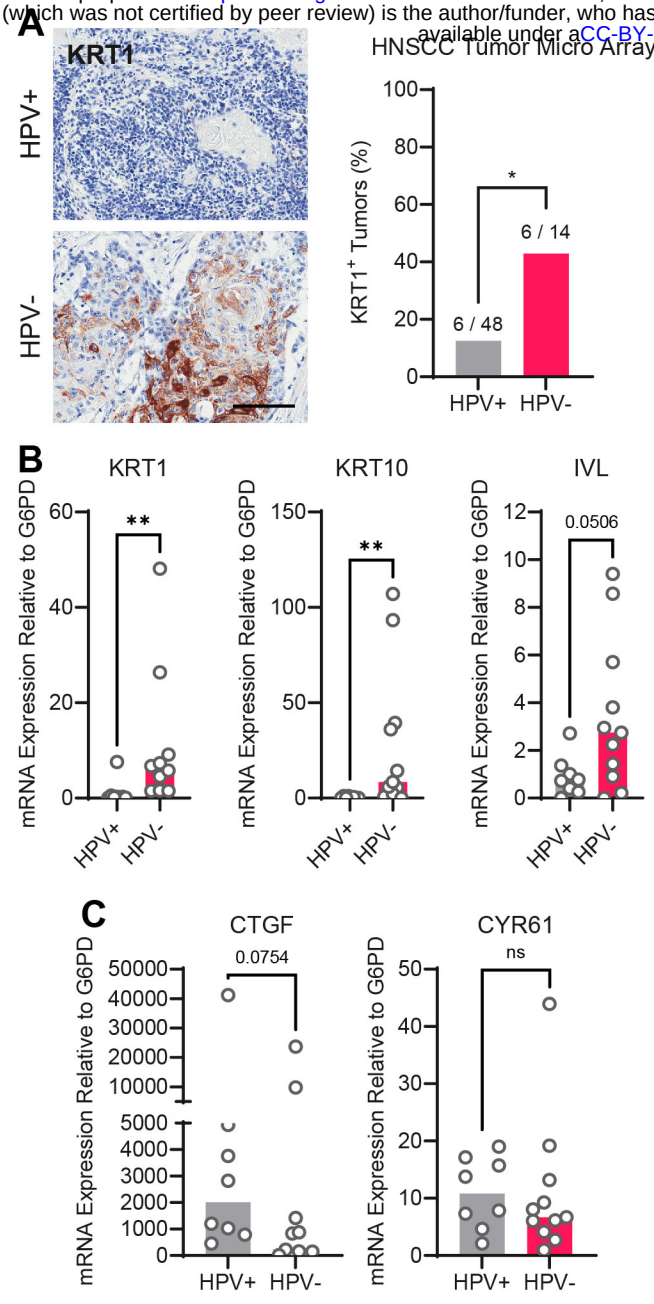

Figure 5 | HPV-positive HNSCC are less differentiated than HPV-negative HNSCC. (A) Human HNSCC tumor samples were stained for KRT1 (left). Scale bar = 100 μm. Graph displays the percentage of tumors that were KRT1+ (right). Statistical significance was determined by Fisher's exact test. (B-C) Total RNA was purified from PDX samples and qRT-PCR was used to assess gene expression of (B) the differentiation markers KRT1, KRT10, and IVL and (C) the canonical YAP1/TAZ targets CTGF and CYR61. Statistical significance was determined by Mann-Whitney nonparametric test. (*p<0.05, **p<0.01, ****p<0.0001).

(Figure 5B). We observed the same pattern of differentiation marker gene expression in an analysis of transcriptomic data from other cohorts (Figure 5—figure supplement 1A-C) (Lawrence et al., 2015). Having confirmed that HPV-positive HNSCC exhibit reduced expression of differentiation markers than do HPV-negative HNSCC, we measured *CTGF* and *CYR61* levels. We found no significant difference in expression of these canonical YAP1/TAZ target genes in HPV-positive vs HPV-negative PDX, although there was a trend towards higher *CTGF* in the HPV-positive PDX (Figure 5C and Figure 5—figure supplement 1D,E). The pattern of low expression of differentiation markers and unchanged canonical YAP1/TAZ target gene expression in HPV-positive versus HPV-negative patient samples is consistent with the effects of PTPN14 inactivation in cultured cells.

High-risk HPV E7 require YAP1/TAZ-TEAD transcriptional activity to extend the lifespan of primary keratinocytes.

High-risk but not low-risk HPV E7 proteins can extend the lifespan of primary keratinocytes (Halbert et al., 1991). The TEADi protein is a genetically encoded competitive inhibitor that prevents binding between YAP1/TAZ and TEAD transcription factors (Yuan et al., 2020). We used TEADi to test whether YAP1/TAZ-TEAD transcriptional activity was required for high-risk HPV E7 to extend the lifespan of primary HFK. We transduced HFK with retroviral vectors encoding GFP, HPV16 E7, or HPV18 E7 plus a lentiviral vector encoding doxycycline-inducible GFP-TEADi. As anticipated, HPV16 E7 or HPV18 E7 extended the lifespan of primary HFK based on cumulative population doublings (Figures 6A,B). TEADi induction upon doxycycline treatment decreased the lifespan of primary HFK in the presence or absence of E7, but the effect of YAP1/TAZ-TEAD inhibition was greater in the HPV16 E7 and HPV18 E7 cells, where E7 had minimal ability to promote growth in the presence of TEADi. We conclude that high-risk HPV E7 proteins require YAP1/TAZ-TEAD transcriptional activity for their lifespan extending capacity in primary keratinocytes.

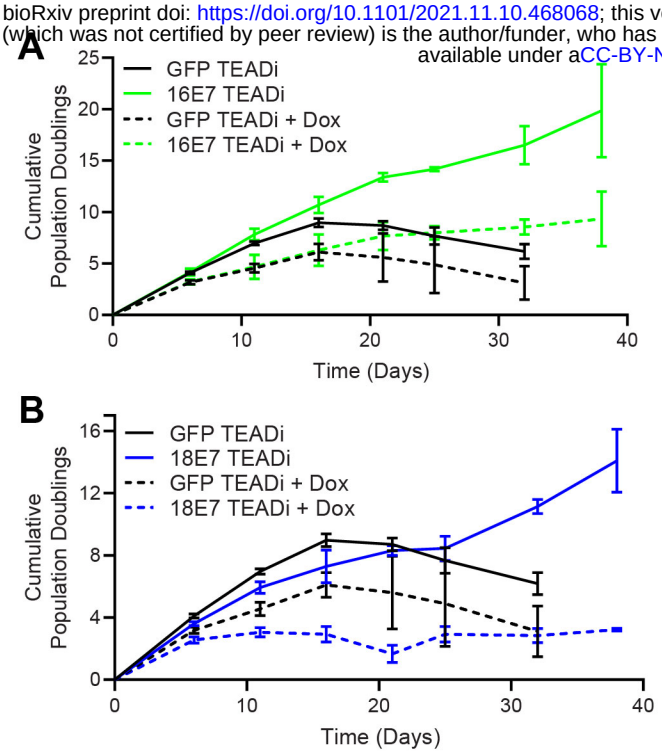

Figure 6 | High-risk HPV E7 requires YAP1/TAZ-TEAD transcriptional activity to extend the lifespan of primary keratinocytes. Primary HFK were transduced with retroviruses encoding HPV16 E7, HPV18 E7, or GFP, plus pInducer20 TEADi lentivirus. Each cell population was cultured with or without 1 μg/mL doxycycline in the media for 38 days and population doublings were tracked with each passage. Graph displays the mean ± SD of two independently transduced cell populations per condition.

PTPN14 loss and YAP1 activation promote basal cell retention in organotypic cultures

YAP1 overexpression impairs differentiation and promotes progenitor cell identity in squamous and non-squamous epithelia. HPV infection is maintained in a reservoir of infected basal cells and productive virus replication begins upon commitment to differentiation. To better understand how repression of differentiation downstream of YAP1 activation affects HPV viral biology, we developed an assay to measure cell retention in the basal epithelial layer. We hypothesized that YAP1 activation by HPV E7 might promote the adoption of a basal cell identity in stratified squamous epithelia. In our cell fate monitoring assay, a small proportion of GFP-labeled cells were mixed with unmodified, parental HFK, and the pool was used to generate organotypic cultures in which normal labeled cells are randomly distributed throughout the epithelium.

Our initial experiment tested whether YAP1 activation altered cell fate in stratified squamous epithelia. We used GFP-labeled tracing cells that expressed doxycycline-inducible YAP1 WT, YAP1 S127A (hyperactive), or YAP1 S94A (cannot bind TEAD transcription factors) (Figure 7—figure supplement 1A,B). In organotypic cultures grown from a 1:25 mixture of GFP-labeled cells and unmodified HFK, about 20% of uninduced GFP+ cells were found in the basal layer. Induction of YAP1 WT or YAP1 S127A expression was sufficient to promote the retention of nearly 60% of labeled cells in the basal layer of the epithelium (Figure 7A,B). Only around 40% of GFP+ cells were found in the basal layer when YAP1 S94A was induced. These data indicate that YAP1 activation causes cells to be retained in the basal layer of a stratified squamous epithelium. The ability of YAP1 to bind TEAD transcription factors contributed to its activity in the cell fate assay.

We next tested whether loss of PTPN14 expression was sufficient to promote basal cell identity. We grew organotypic cultures from mixtures of unmodified primary HFK and GFP-labeled control or PTPN14 KO HFK (Figure 7—figure supplement 1C,D). 60-70% of PTPN14 KO tracer cells were found in the basal layer when either of two PTPN14 guide RNAs were used whereas

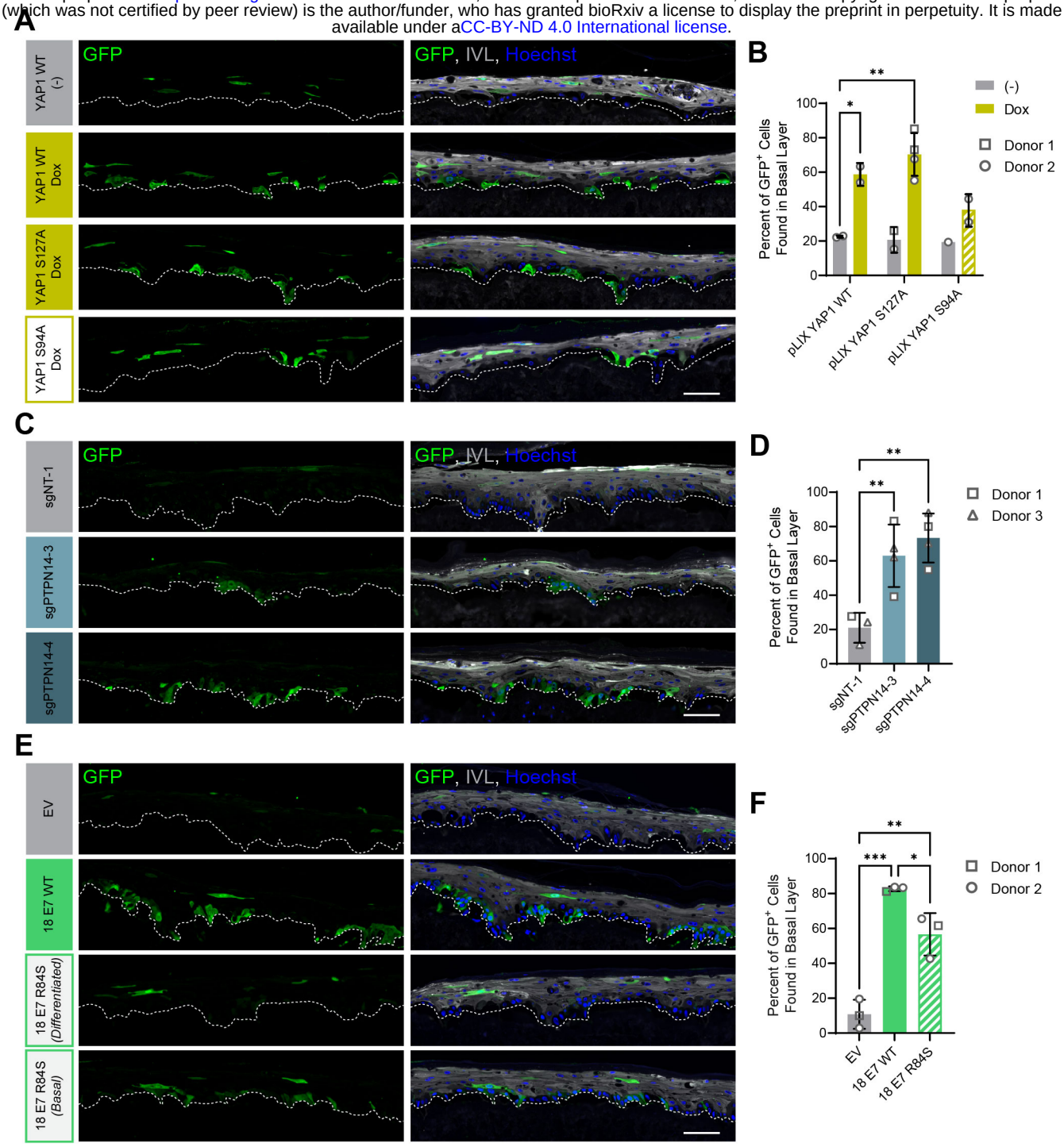

Figure 7 | PTPN14 loss and YAP1 activation by HPV E7 promote basal cell retention in organotypic cultures. Organotypic cultures were grown from GFP-labeled HFK mixed with unmodified HFK. (A-B) GFP-labeled HFK were transduced with lentiviral vectors encoding YAP1 WT, YAP1 S127A, or YAP1 S94A under the control of a doxycycline inducible promoter. GFP-labeled YAP1 cells were mixed 1:25 into unmodified HFK and organotypic cultures were grown from the mixture. Cultures were grown +/- 1 µg/mL doxycycline. (C-D) GFP-labeled HFK were transduced with LentiCRISPR v2 vectors encoding control or PTPN14 targeting sgRNAs. GFP-labeled cells were mixed 1:25 into unmodified HFK and organotypic cultures were grown from the mixture. (E-F) GFP-labeled HFK were transduced with HPV18 E7 WT, HPV18 E7 R84S, or the empty vector (EV). GFP-labeled HPV18 E7 cells were mixed 1:50 into unmodified HFK and organotypic cultures were grown from the mixture. (A, C, E) FFPE sections of cultures were stained for GFP (green), IVL (grey), and Hoechst (blue). Scale bar = 100 µm. (B, D, F) Quantification of the percentage of GFP+ cells found in the basal layer. Graphs display the mean ± SD and each individual data point (independent cultures). Shapes indicate cultures grown from different HFK donors. Statistical significance was determined by ANOVA. (*p<0.05, **p<0.01).

about 20% of control tracer cells were retained in the basal layer (Figure 7C,D). Thus, PTPN14 knockout is sufficient to promote basal cell fate determination in keratinocytes.

Next, we tested whether HPV E7 promoted basal cell retention and if so, whether its cell retention activity required PTPN14 degradation. We grew organotypic cultures from mixtures of GFP-labeled HFK expressing HPV18 E7 WT, HPV18 E7 R84S, or the empty vector control diluted 1:50 into unmodified primary HFK (Figure 7—figure supplement 1E,F). We found that nearly 80% of GFP-labeled HPV18 E7 WT tracer cells were retained in the basal layer compared to about 10% of labeled control cells (Figure 7E,F). HPV18 E7 WT labeled cells were numerous and grouped in clusters in the basal layer, suggesting that E7 promoted the clonal expansion of labeled basal cells. Both effects were dampened in experiments using HPV18 E7 R84S tracer cells (cannot degrade PTPN14). Labeled HPV18 E7 R84S cells exhibited varying degrees of basal cell expansion and basal cell retention and approximately 60% of labeled cells were in the basal layer. HPV18 E7 R84S retains the ability to inactivate RB1 and we interpret these data to mean that the proliferation of labeled basal cells resulted from RB1 inactivation. Finally, HPV18 E7 ΔDLLC cannot bind RB1 but can bind and degrade PTPN14. In a cell fate experiment using GFP-labeled HPV18 E7 ΔDLLC tracer cells, the labeled cells were present mainly as single cells in the basal layer (Figure 7—figure supplement 2A-B). The behavior of the two mutant HPV E7 proteins supports that PTPN14 degradation is required for basal cell retention and RB1 inactivation is required for basal cell expansion. We conclude that PTPN14 degradation and YAP1 activation by HPV18 E7 promote basal cell retention.

Discussion

YAP1 and TAZ are oncogenes that promote growth and inhibit differentiation in stratified squamous epithelia (Elbediwy et al., 2016; Schlegelmilch et al., 2011; Totaro et al., 2017; Yuan et al., 2020; Zhang et al., 2011). Here we report that HPV E7 activates YAP1 (Figure 1). YAP1/TAZ-TEAD transcriptional activity is required for the carcinogenic activity of HPV E7 (Figure

6) and YAP1 activation by E7 biases HPV E7-expressing cells to be retained in the basal epithelial layer (Figure 7). Based on these findings we propose that YAP1 activation by HPV E7 enables HPV-infected cells to persist in stratified epithelia. There is substantial evidence that RB1 inactivation is necessary but insufficient for the transforming activity of high-risk HPV E7 (Balsitis et al., 2006, 2005; Banks et al., 1990; Ciccolini et al., 1994; Helt and Galloway, 2002; Huh et al., 2005; Ibaraki et al., 1993; Jewers et al., 1992; Phelps et al., 1992; Strati and Lambert, 2007; White et al., 2015). We propose that YAP1 activation cooperates with RB1 inactivation to enable the transforming activity of HPV E7.

PTPN14 binding by HPV18 E7 was required for activation of YAP1 in the basal layer and PTPN14 KO was sufficient for the same effect (Figure 2). Highly conserved amino acids in E7 participate in binding to PTPN14 (Hatterschide et al., 2020; Yun et al., 2019), indicating that YAP1 activation and maintenance of basal cell state is likely shared among diverse papillomavirus E7 proteins. Some minor genotype-specific differences were apparent. HPV18 E7 depletes PTPN14 protein levels more efficiently than HPV16 E7 (Hatterschide et al., 2020; White et al., 2016), which is consistent with the observed stronger effect of HPV18 E7 on YAP1 nuclear localization in basal cells (Figure 1). Genotype-specific differences could also explain the stronger effect of TEADi on HPV18 E7 in lifespan extension assays (Figure 6). Although other reports have suggested that HPV might activate YAP1 (He et al., 2015; Morgan et al., 2020; Olmedo-Nieva et al., 2020; Webb Strickland et al., 2018), no specific activity of an HPV protein has previously been shown to enable YAP1 activation. Other groups have proposed that HPV E6 activates YAP1 (He et al., 2015; Webb Strickland et al., 2018), but we did not observe YAP1 activation by HPV E6. We conclude that activation of YAP1 by HPV E7 is contingent upon its ability to bind and degrade PTPN14.

Even when HPV E7 was expressed in all layers of a stratified epithelium, YAP1 levels and nuclear localization increased only in basal epithelial cells. We found that E7 required PTPN14 degradation to activate YAP1 and that PTPN14 was expressed predominantly in basal keratinocytes (Figure 3). Basal cell-specific expression of *PTPN14* is consistent with the

observation that it is regulated by p63, the master regulator of basal cell identity in stratified epithelia (Perez et al., 2007). We propose that PTPN14 inhibits YAP1 primarily in basal cells and that unlike the effects of E7 on RB1 in both differentiated and undifferentiated cells, E7 activates YAP1 primarily in basal cells.

Degradation of PTPN14 by HPV E7 represses keratinocyte differentiation but does not induce canonical Hippo pathway target genes (Hatterschide et al., 2020, 2019). Nonetheless, we found that PTPN14 overexpression promoted differentiation only in the presence of YAP1/TAZ (Figure 4C,D). Few studies have tested how YAP1 inhibitor inactivation alters gene expression downstream of YAP1. Here we demonstrate that inactivation of LATS1 or LATS2, two well-characterized inhibitors of YAP1/TAZ, also repressed differentiation genes but did not induce canonical YAP1/TAZ targets (Figure 4E-I). Taken together, these experiments indicate that PTPN14 acts through YAP1/TAZ to regulate differentiation in keratinocytes. It is so far unclear why *CTGF* and *CYR61* expression is sensitive to large changes in total levels of YAP1 or TAZ yet is unaffected by alterations in regulators upstream of YAP1/TAZ. Nonetheless, the pattern of low differentiation gene expression and unchanged expression of canonical YAP1/TAZ target genes caused by PTPN14 loss is consistent with gene expression differences between HPV-positive and HPV-negative HNSCC.

PTPN14 knockout and knockdown reduced differentiation gene expression in monolayer culture. Even so, we did not observe reduced differentiation in suprabasal layers of organotypic cultures grown from PTPN14 knockout cells (Figure 2A and Figure 2—figure supplement 1A-C). Using our cell fate monitoring assay, we determined that instead, HPV18 E7 promotes basal cell retention and that either YAP1 overexpression or PTPN14 KO are sufficient for this activity (Figure 7). The effect of YAP1 activation on cell fate in our assay resembles several experiments in which YAP1 promotes progenitor cell identity in airway and liver epithelia (Yimlamai et al., 2014; Zhao et al., 2014). Our findings demonstrate that YAP1 activation enables basal cell fate determination in stratified squamous epithelia and show that loss of an inhibitor of YAP1 has the same effect.

We conclude that one consequence of YAP1 activation by HPV E7 is that E7-expressing cells are retained in the basal layer of stratified squamous epithelia.

Although persistent infection is a prerequisite for HPV-mediated carcinogenesis, the mechanisms used by papillomaviruses to establish persistent infections remain incompletely understood. Maintaining infection in the basal cell compartment is critical for papillomavirus persistence. Substantial effort has been devoted to the mechanistic understanding of how the papillomavirus genome is stably maintained in the basal layer upon cell division. However, much less is known about how papillomaviruses manipulate epithelial cell fate to establish and expand the pool of infected basal cells. Previously, HPV E7 was believed to be primarily required to establish a cellular environment conducive to HPV DNA replication in suprabasal cells. We propose that a so far unappreciated role of E7 is that it activates YAP1 to facilitate HPV persistence by biasing infected cells to remain in the basal layer of the epithelium. Not every HPV E7-expressing cell was retained in the basal layer, so we do not anticipate that YAP1 activation would block differentiation-dependent HPV replication. HPV E6 also represses differentiation gene expression in keratinocytes and has been proposed to promote basal cell retention (Kranjec et al., 2017). Further research is needed to determine the extent to which different HPV genotypes depend on the activities of E6 or E7 for basal cell retention activity.

To the best of our knowledge, no other viruses are recognized to modulate cell fate decisions in solid tissues in a way that facilitates persistence. Some herpesviruses impact the choice between progenitor/differentiated cell fates in infected immune cells, for example Epstein-Barr Virus (EBV) restricts B-cell differentiation to facilitate viral latency (Knox and Carrigan, 1992; Niiya et al., 2006; Onnis et al., 2012; Romeo et al., 2019; Styles et al., 2017). Herpesviruses, polyomaviruses, and hepadnaviruses encode proteins proposed to activate YAP1/TAZ or alter Hippo signaling (Hwang et al., 2014; Liu et al., 2014, 2015; Nguyen et al., 2014; Shanzer et al., 2015; Tian et al., 2004; Z. Wang et al., 2020). Not all of the mechanisms used by these viruses to activate YAP1 nor the downstream consequences of YAP1 activation have been well defined.

Our finding that HPV E7 activates YAP1 to manipulate cell fate opens up an exciting new line of inquiry into how YAP1, TAZ, and the Hippo signaling pathway could impact viral infections by regulating tissue developmental processes.

YAP1 activation and PTPN14 are relevant to both viral and non-viral cancers. We found that a genetically encoded inhibitor of YAP1/TAZ-TEAD transcription inhibited the growth of high-risk HPV E7 expressing cells (Figure 6), indicating that high-risk HPV E7 proteins require YAP1 or TAZ for carcinogenesis. YAP1/TAZ activation is sufficient to drive carcinogenesis in mouse models of cervical and oral cancer (He et al., 2019; Nishio et al., 2020; Omori et al., 2020), and the YAP1 inhibitor verteporfin reduced the growth of HPV-positive tumors in a xenograft model (Liu et al., 2019). YAP1 activation correlates with the clinical stage of HPV infection (Nishio et al., 2020), and YAP1 localizes to the nucleus in HPV-positive cancers (Alzahrani et al., 2017). Basal cell carcinoma (BCC) is the non-viral cancer that is most clearly linked to PTPN14. Germline inactivating mutations in *PTPN14* are associated with a 4- to 8-fold increase in risk of BCC by age 70 (Olafsdottir et al., 2021) and somatic mutations in *PTPN14* are frequent in BCC (Bonilla et al., 2016). YAP1/TAZ-TEAD transcriptional activity also restricts differentiation in BCC cells (Yuan et al., 2021). We propose that the specific association of PTPN14 with BCC is related to our observation that PTPN14 loss activates YAP1 in basal epithelial cells. YAP1 inhibition is of major clinical interest for several cancer types, and it is appealing to speculate that targeting YAP1 could treat persistent HPV infection and/or HPV-positive cancers.

Materials and Methods

Plasmids and cloning. pInducer20 EGFP-TEADi was a gift from Ramiro Iglesias-Bartolome (Addgene plasmid # 140145) (Yuan et al., 2020). pQCXIH-Myc-YAP (Addgene plasmid # 33091), pQCXIH-Flag-YAP-S127A (Addgene plasmid # 33092), and pQCXIH-Myc-YAP-S94A (Addgene plasmid # 33094) were gifts from Kun-Liang Guan (Zhao et al., 2007). Each YAP1 ORF was amplified by PCR from pQCXIH, cloned into pDONR223, and transferred into pLIX_402 lentiviral backbone using Gateway recombination. pLIX_402 was a gift from David Root (Addgene plasmid # 41394). pLenti CMV GFP Hygro (656-4) was a gift from Eric Campeau & Paul Kaufman (Addgene plasmid # 17446) (Campeau et al., 2009). PHAGE-P-CMVt N-HA GFP was previously described (Galligan et al., 2014). pNeo-loxP-HPV18 was the kind gift of Thomas Broker and Louise Chow (Wang et al., 2009). The ΔDLLC mutation was introduced into the pDONR HPV18 E7 vector using site-directed mutagenesis. HPV18 E7 ΔDLLC and GFP ORFs were cloned into MSCV-P C-FlagHA GAW or MSCV-Neo C-HA GAW destination vectors using Gateway recombination. The remaining MSCV-P C-FlagHA and MSCV-Neo C-HA HPV E6 and HPV E7 retroviral plasmids and pHAGE lentiviral plasmids have been previously described (Hatterschide et al., 2020; White et al., 2016, 2012a, 2012b). A complete list of all plasmids used in this study is in Supplemental File 1.

Cell culture, retrovirus production, and lentivirus production. Deidentified primary human foreskin keratinocytes (HFK) and human foreskin fibroblasts (HFF) were provided by the University of Pennsylvania Skin Biology and Disease Resource-Based Center (SBDRC). N/Tert-1 cells are hTert-immortalized HFK (Dickson et al., 2000), and N/Tert-Cas9 mock and sgPTPN14-1 are N/Tert-1 cells further engineered to constitutively express Cas9 (Hatterschide et al., 2019). Keratinocytes for cell fate experiments were cultured in keratinocyte serum-free media (KSFM) (Life Technologies, Carlsbad, California) mixed 1:1 with Medium 154 (Thermo Fisher Scientific, Waltham, Massachusetts) with the human keratinocyte growth supplement (HKGS) (Thermo

Fisher Scientific) (Duperret et al., 2015; Egolf et al., 2019). Keratinocytes for all other experiments were cultured as previously described (White et al., 2012a). HFF were cultured in Dulbecco's Modified Eagle Medium (DMEM) (Thermo Fisher Scientific) supplemented with antibiotic and antimycotic. HFK harboring the HPV18 genome were previously described (Hatterschide et al., 2020), and were generated by transfecting cells with the pNeo-loxP-HPV18 vector (Wang et al., 2009) along with NLS-Cre and selecting with G418 to generate a stable population. Lentiviruses and retroviruses were produced in 293T or 293 Phoenix cells respectively as previously described (White et al., 2016). Stable keratinocyte populations were generated following transduction by selection with puromycin, G418, or hygromycin alone or in combination.

Lifespan extension assay. Primary HFK were engineered and cultured as described in cell culture, retrovirus production, and lentivirus production. The growth of engineered HFK was monitored in culture for 38 days. Population doublings were calculated using the number of cells at the beginning and end of each passage.

Organotypic epithelial culture. Devitalized human dermis was provided as deidentified material from the University of Pennsylvania SBDRC. Stands for organotypic epithelial cultures were printed using high temperature, autoclavable resin at the University of Pennsylvania Biotech Commons 3D-printing facility. Organotypic cultures were generated as previously described (Duperret et al., 2015; Egolf et al., 2019). Devitalized dermis was seeded with primary HFF on the dermal side at a density of 3×10^4 cells per cm^2 of culturing area and cultured for four days. Dermis and fibroblasts were then stretched across 3D-printed stands. The epidermal side of the dermis was seeded with unmodified or engineered keratinocytes at a density of 1×10^6 cells per cm^2. Organotypic cultures were cultured in E media (Fehrmann and Laimins, 2005) with the dermal layer maintained at the air-liquid interface starting on the day of seeding keratinocytes. Cultures were allowed to stratify for 12-14 days, then trimmed and fixed in 10% neutral buffer

formalin for 24 hours. Tissues were embedded in paraffin and sectioned by the SBDRC Core A. A complete list of all organotypic cultures used in this study is in Supplemental File 2.

siRNA transfection. Primary HFK were transfected with siRNAs using the Dharmafect 1 transfection reagent. All siRNA experiments were collected 72 h post transfection. Two siRNAs were used to target each gene in an experiment. The siRNAs used in this study were all purchased from Dharmacon (Lafayette, Colorado): nontargeting siRNA, siYAP1-06, siYAP1-08, siWWTR1-06, siWWTR1-08, siPTPN14-05, siPTPN14-08, siLATS1-05, siLATS1-08, siLATS2-09, siLATS2-10.

Laser capture microdissection. Formalin-fixed paraffin-embedded (FFPE) organotypic cultures were sectioned onto polyethylene naphthalate (PEN) membrane glass slides by the SBDRC Core A. Laser capture microdissection was performed on a Leica LMD 7000 microscope. Hundreds of microdissections were made per sample amounting to ~1.5 mm^2 of total dissected area per sample. RNA was isolated using the RNeasy FFPE kit (Qiagen, Germantown, Maryland). RNA concentration was determined using Qubit RNA HS assay kit (Life Technologies).

Patient derived xenografts. The PDXs were previously established from surgical resections of treatment-naive HPV-positive OPSCC as described (Facompre et al., 2020). Human tumors were engrafted subcutaneously in NSG mice and passaged at least twice before cryopreservation when they reached a volume of 0.5-1.0 cm^3. Total tumor RNA was isolated using the QIAamp RNA Blood Mini Kit (Qiagen).

Western blotting. Western blots were performed using Mini-PROTEAN (Bio-Rad Laboratories, Hercules, California) or Criterion (Bio-Rad) Tris/Glycine SDS-PAGE gels and transfers were performed onto polyvinylidene difluoride (PVDF). Membranes were blocked with 5% nonfat dried

492 milk in Tris-buffered saline with 0.05% Tween 20 (TBST). Membranes were incubated with
493 primary antibodies as specified in Supplemental File 1. Following TBST washes, membranes
494 were incubated with horseradish peroxidase-coupled secondary antibodies and imaged using
495 chemiluminescent substrate on an Amersham Imager 600 (GE Healthcare, Chicago, Illinois).
496
497 **qRT-PCR.** Unless otherwise specified, total cellular RNA was isolated using the NucleoSpin RNA
498 extraction kit (Macherey-Nagel/Takara, San Jose, California). cDNA was generated from bulk
499 RNA with the high-capacity cDNA reverse transcription kit (Applied Biosystems, Waltham,
500 Massachusetts). cDNAs were used as a template for qPCR using Fast SYBR green master mix
501 (Applied Biosystems) and a QuantStudio 3 system (Thermo Fisher Scientific). 18S rRNA qRT-
502 PCR primers were ordered from Integrated DNA Technologies (Integrated DNA Technologies,
503 Inc., Coralville, Iowa): FWD, 5- CGCCGCTAGAGGTGAAATTCT; REV, 5-
504 CGAACCTCCGACTTTCGTTCT (Roh et al., 2005). KiCqStart SYBR green primers for qRT-PCR
505 (MilliporeSigma, St. Louis, Missouri) were used for the remaining genes assayed in this study:
506 KRT1, KRT10, IVL, ITGB4, ITGA6, CYR61, CTGF, PTPN14, YAP1, WWTR1, LATS1, LATS2,
507 G6PD, and GAPDH.
508
509 **Immunofluorescence, immunohistochemistry, and microscopy.** FFPE sections were
510 prepared for immunofluorescence by deparaffinization with xylene washes, rehydration through
511 an ethanol gradient, and heat induced epitope retrieval (HIER). Tissue sections were blocked with
512 PBS containing 1% bovine serum albumin, 10% normal goat serum, and 0.3% Triton X-100.
513 Tissue sections were incubated with primary antibodies at 4°C overnight, washed with PBS with
514 0.05% Tween 20, and incubated with fluorescently labeled secondary antibodies and Hoechst
515 33342 at room temperature. Antibody dilutions and HIER conditions are specified in Supplemental
516 File 1. Fluorescent micrographs were captured using an Olympus IX81 microscope. All

fluorescent micrograph images within the same figure panels were captured using the same exposure time and batch processed using the same contrast settings.

The TMA was constructed from surgical resection specimens of 120 HNSCC that vary by TNM stage and HPV status (Supplemental File 3). Archival FFPE tumors of the oral cavity and oropharynx were identified retrospectively and oropharyngeal tumors were evaluated for HPV status as per College of American Pathologists criteria (Lewis et al., 2018) using IHC for p16. When present, lymph node metastases were included in association with the primary tumor of origin. All FFPE specimens were represented in the TMA by at least three tissue cores that incorporate both non-necrotic central tumor regions and invasive margins. Tumor materials and clinical data were accessed under University of Pennsylvania IRB protocol 417200. Staining for KRT1 was performed by the Clinical Services Laboratory in the University of Pennsylvania Department of Pathology and Laboratory Medicine. Antibody information can be found in Supplemental File 1. The KRT1 stained slides were reviewed with a standard light microscope, and evaluation was based on the presence or absence of staining in the cytoplasm of tumor cells.

Bioinformatic analysis. Genomic mutation and copy number variation data as well as tumor RNA-seq gene expression data from TCGA (Lawrence et al., 2015) were analyzed using the cBioPortal.org graphical interface (Cerami et al., 2012; Gao et al., 2013). RNA-seq V2 RSEM (RNA-Seq by Expectation Maximization) normalized expression values for individual genes were downloaded directly from cBioPortal.org. OPSCC were distinguished from HNSCC by clinical annotation of primary tumor site and HPV-positive and HPV-negative status was assigned based on previously reported HPV transcript status (Chakravarthy et al., 2016). Genes included as a part of each pathway analysis are listed in Supplemental File 4. Missense, truncating, and splice mutations of unknown significance as well as amplifications of tumor suppressor genes and deletion of oncogenes were excluded from total alteration tallies.

Single cell-RNA sequencing dataset derived from the human neonatal foreskin epidermis and subsequent clustering analysis were retrieved from GitHub (S. Wang et al., 2020) and reanalyzed with MATLAB. PTPN14 expression was calculated by averaging mRNA expression for all cells by cluster and donor.

Acknowledgments

We thank the members of our laboratories, particularly Pavithra Rajagopalan, for helpful discussions. We thank Stephen M. Prouty, Ph.D. from the SBDRC for help with tissue processing and sectioning. Stands for organotypic cultures were printed courtesy of the University of Pennsylvania Libraries' Biotech Commons. This work was supported by American Cancer Society grant 131661-RSG-18-048-01-MPC and NIH/NIAID R01 AI148431 to EAW. DB is supported by NIH/NIDCR R01 DE027185. JH was supported by NIH/NIAID T32 AI007324 and NIH/NIDCR F31 DE030365. SBDRC was funded by NIH grant P30 AR068589.

Author Contributions

Conception and design: JH, EAW. Acquisition of data: JH, PC, HWK, KTM, EAW. Analysis and interpretation of data: JH, PC, KTM, DB, EAW. Drafting or revising the article: JH, PC, DB, EAW. Contributing unpublished essential data or reagents: SMS, KTM, DB.

Figure Legends

Figure 1 | HPV E7 activates YAP1 in basal epithelial keratinocytes. (A) cBioPortal analysis for total genomic mutations and copy number alterations in HPV+/- OPSCC and HNSCC. Graph displays the percent of tumors with alterations in each pathway. Statistical significance was determined by Fisher's exact test. (B-D) Organotypic cultures were grown from primary HFK, HFK harboring the HPV18 genome, or HFK transduced with retroviral expression encoding HPV E6 or E7 proteins. FFPE sections of cultures grown from (C) HFK or HFK harboring the HPV18 genome, (D) HFK or HFK expressing HPV16 E7 or HPV18 E7, or (E) HFK or HFK expressing HPV16 E6 or HPV16 E7 were stained for YAP1 (magenta), PCNA (green), and Hoechst (gray). White dashed lines indicate the basement membrane. White boxes indicate the location of insets in main images. Main image scale bars = 100 μm. Inset scale bars = 25 μm.

Figure 2 | HPV E7 activates YAP1 in basal keratinocytes through PTPN14 degradation. Organotypic cultures were grown from N/Tert-Cas9 keratinocytes or primary HFK transduced with retroviral expression vectors encoding HPV18 E7 WT or R84S. (A) FFPE sections of cultures grown from mock or sgPTPN14 transfected N/Tert-Cas9 keratinocytes were stained for YAP1 (magenta), IVL (green), and Hoechst (Gray). (B) FFPE sections of cultures grown from parental HFK, HPV18 E7 WT or HPV18 E7 R84S expressing HFK were stained for YAP1 (magenta), PCNA (green), and Hoechst (Gray). White dashed lines indicate the basement membrane. White boxes indicate the location of insets in main images. Main image scale bars = 100 μm. Inset scale bars = 25 μm. (C-F) Quantification of the number of (C and E) basal cells and (D and F) suprabasal cells per 100 μm of epidermis. Graphs display the mean ± SD and each individual data point (independent cultures). Statistical significance was determined by ANOVA (*$p<0.05$, ***$p<0.001$).

Figure 3 | PTPN14 expression is enriched in basal keratinocytes. (A-B) Single-cell RNA sequencing data and clustering analysis from Wang et al. was reanalyzed to assess PTPN14

586 expression in different subsets of epidermal cells. (A) Diagram of epidermis; shading depicts
587 tissue localization of cell clusters. (B) For each donor, the mean of PTPN14 mRNA expression
588 was calculated for each cell cluster. Graphs display the mean of PTPN14 mRNA expression for
589 each donor (circles) as well as the mean of all five donors ± SEM (bars and error bars). Statistical
590 significance was determined by ANOVA (*p<0.05, **p<0.01). (C-F) Basal and suprabasal layers
591 from organotypic cultures were dissected using laser capture microdissection. (C) Representative
592 images of HFK cultures before and after individual laser dissections. Hundreds of such cuts were
593 performed per sample. (D-F) RNA was purified from isolated layers and qRT-PCR was used to
594 assess the expression of PTPN14 (D), basal cell markers ITGA6 and ITGB4 (E), and
595 differentiation markers KRT1 and IVL (F). Graphs display the mean and each individual data point.
596
597 **Figure 4 | YAP1/TAZ regulate differentiation downstream of PTPN14.** (A) Venn diagram
598 comparing the MSigDB YAP conserved signature to the differentially expressed genes (DEG)
599 from our two published experiments that reflect PTPN14 loss in keratinocytes. (B-D) *YAP1* and
600 *WWTR1* were simultaneously knocked down by siRNA transfection in HFK. Transfected HFK
601 were then transduced with PTPN14 lentivirus at 24h post transfection. Cells were lysed for protein
602 and total cellular RNA at 72h post transfection. (B) Cell lysates were subjected to
603 SDS/PAGE/Western analysis and probed with antibodies to PTPN14, YAP1, TAZ, and Actin. (C
604 and D) qRT-PCR was used to measure the expression of the differentiation markers *KRT1* and
605 *IVL* relative to *G6PD*. Graphs display fold change in gene expression relative to the mock
606 transduced cells. (E-I) Primary HFK were transfected with siRNAs targeting *YAP1*, *WWTR1*
607 (TAZ), *PTPN14*, *LATS1*, and *LATS2*. Two siRNAs were used per target. qRT-PCR was used to
608 measure gene expression for: the differentiation markers *IVL* (E) and *KRT1* (F), and the canonical
609 YAP1/TAZ targets *CTGF* (G) and *CYR61* (H). Data confirming that individual siRNA transfections
610 depleted intended transcripts is summarized in a heatmap of $\log_2$(fold-change) levels (I). Bar

graphs display the mean ± SD of three independent replicates. Statistical significance was determined by ANOVA (*p<0.05, **p<0.01, ***p<0.001, ****p<0.0001).

Figure 5 | HPV-positive HNSCC are less differentiated than HPV-negative HNSCC. (A) Human HNSCC tumor samples were stained for KRT1 (left). Scale bar = 100 μm. Graph displays the percentage of tumors that were KRT1^{+} (right). Statistical significance was determined by Fisher's exact test. (B-C) Total RNA was purified from PDX samples and qRT-PCR was used to assess gene expression of (B) the differentiation markers KRT1, KRT10, and IVL and (C) the canonical YAP1/TAZ targets CTGF and CYR61. Statistical significance was determined by Mann-Whitney nonparametric test. (*p<0.05, **p<0.01, ****p<0.0001).

Figure 6 | High-risk HPV E7 requires YAP1/TAZ-TEAD transcriptional activity to extend the lifespan of primary keratinocytes. Primary HFK were transduced with retroviruses encoding HPV16 E7, HPV18 E7, or GFP, plus pInducer20 TEADi lentivirus. Each cell population was cultured with or without 1 μg/mL doxycycline in the media for 38 days and population doublings were tracked with each passage. Graph displays the mean ± SD of two independently transduced cell populations per condition.

Figure 7 | PTPN14 loss and YAP1 activation by HPV E7 promote basal cell retention in organotypic cultures. Organotypic cultures were grown from GFP-labeled HFK mixed with unmodified HFK. (A-B) GFP-labeled HFK were transduced with lentiviral vectors encoding YAP1 WT, YAP1 S127A, or YAP1 S94A under the control of a doxycycline inducible promoter. GFP-labeled YAP1 cells were mixed 1:25 into unmodified HFK and organotypic cultures were grown from the mixture. Cultures were grown +/- 1 μg/mL doxycycline. (C-D) GFP-labeled HFK were transduced with LentiCRISPR v2 vectors encoding control or PTPN14 targeting sgRNAs. GFP-

636 labeled cells were mixed 1:25 into unmodified HFK and organotypic cultures were grown from the
637 mixture. (E-F) GFP-labeled HFK were transduced with HPV18 E7 WT, HPV18 E7 R84S, or the
638 empty vector (EV). GFP-labeled HPV18 E7 cells were mixed 1:50 into unmodified HFK and
639 organotypic cultures were grown from the mixture. (A, C, E) FFPE sections of cultures were
640 stained for GFP (green), IVL (grey), and Hoechst (blue). Scale bar = 100 μm. (B, D, F)
641 Quantification of the percentage of GFP+ cells found in the basal layer. Graphs display the mean
642 ± SD and each individual data point (independent cultures). Shapes indicate cultures grown from
643 different HFK donors. Statistical significance was determined by ANOVA. (*p<0.05, **p<0.01).
644
645 **Figure 1—figure supplement 1 | HPV-positive HNSCC have fewer Hippo pathway**
646 **alterations and lower expression of differentiation genes.** cBioPortal analysis for genomic
647 mutations and copy number alterations in HPV+/- HNSCC and OPSCC. Oncoprint displays
648 specific genomic alterations in individual tumor samples.
649
650 **Figure 1—figure supplement 2 | HPV18 E7 activates YAP1 in basal keratinocytes.** (A-B)
651 Additional replicates of organotypic cultures grown from primary HFK or HFK harboring the
652 HPV18 genome. FFPE sections were stained for YAP1 (magenta), PCNA (green), and Hoechst
653 (gray). White dashed lines indicate the basement membrane. White boxes indicate the location
654 of insets in main images. Main image scale bars = 100 μm. Inset scale bars = 25 μm.
655
656 **Figure 1—figure supplement 3 | HPV E7 activates YAP1 in basal keratinocytes.** Additional
657 replicates of organotypic cultures grown from primary HFK or HFK transduced with retroviral
658 expression encoding HPV E7 proteins. FFPE sections of cultures grown from (A) HFK or HFK
659 expressing HPV16 E7 or HPV18 E7, (B) HFK or HFK transduced with HPV16 E7, or (E) HFK and
660 HFK expressing HPV18 E7 were stained for YAP1 (magenta), PCNA (green), and Hoechst (gray).

White dashed lines indicate the basement membrane. White boxes indicate the location of insets in main images. Main image scale bars = 100 μm. Inset scale bars = 25 μm.

Figure 1—figure supplement 4 | HPV E6 does not activate YAP1 in basal keratinocytes. Additional replicates of organotypic cultures grown from primary HFK or HFK transduced with retroviral expression encoding HPV E6 or E7 proteins. FFPE sections were stained for YAP1 (magenta), PCNA (green), and Hoechst (gray). White dashed lines indicate the basement membrane. White boxes indicate the location of insets in main images. Main image scale bars = 100 μm. Inset scale bars = 25 μm.

Figure 2—figure supplement 1 | PTPN14 knockout activates YAP1 in basal keratinocytes. Additional replicates of organotypic cultures grown from N/Tert-Cas9 keratinocytes (A-C) FFPE sections from mock or sgPTPN14 transfected N/Tert-Cas9 keratinocytes were stained for YAP1 (magenta), IVL (green), and Hoechst (Gray). White dashed lines indicate the basement membrane. White boxes indicate the location of insets in main images. Main image scale bars = 100 μm. Inset scale bars = 25 μm.

Figure 2—figure supplement 2 | HPV E7 activates YAP1 in basal keratinocytes through PTPN14 degradation. Additional replicates of organotypic cultures grown from primary HFK transduced with retroviral expression vectors encoding HPV18 E7 WT or R84S. FFPE sections from parental HFK, HPV18 E7 WT or HPV18 E7 R84S expressing HFK were stained for YAP1 (magenta), PCNA (green), and Hoechst (Gray). White dashed lines indicate the basement membrane. White boxes indicate the location of insets in main images. Main image scale bars = 100 μm. Inset scale bars = 25 μm.

686 **Figure 3—figure supplement 1 | PTPN14 expression is enriched in basal keratinocytes in**
687 **HPV 18 E7 expressing organotypic cultures.** Basal and suprabasal layers from a 3D
688 organotypic culture grown from HFK transduced with a retroviral expression vector encoding
689 HPV18 E7 were dissected using laser capture microdissection. RNA was purified from isolated
690 layers and qRT-PCR was used to assess the expression of PTPN14 (A), the basal cell markers
691 ITGA6 and ITGB4 (B), and the differentiation marker IVL (C). Graphs display individual data
692 points.
693
694 **Figure 4—figure supplement 1 | PTPN14 overexpression promotes differentiation in**
695 **keratinocytes.** NTert-Cas9 Mock and sgPTPN14-1 keratinocytes were transduced with
696 lentiviruses encoding GFP or PTPN14 or the empty vector control. (A) Cell lysates were subjected
697 to SDS/PAGE/Western analysis and probed with antibodies to PTPN14, V5-tag, Involucrin, and
698 Actin. (B) qRT-PCR was used to measure the expression of the differentiation markers IVL and
699 KRT10 relative to G6PD. Graphs display the mean ± SD of two independent replicates.
700
701 **Figure 4—figure supplement 2 | YAP1 and TAZ are required for PTPN14 to promote**
702 **keratinocyte differentiation.** Primary HFK were transfected with control or YAP1 and WWTR1
703 targeting siRNAs then transduced with PTPN14 encoding lentivirus. qRT-PCR was used to
704 measure the expression of the differentiation markers (A) KRT1 and (B) IVL relative to G6PD.
705 Graphs portray the change in gene expression relative to siC. Graphs display the mean ± SD of
706 three independent replicates. Statistical significance was determined by ANOVA (**p<0.01,
707 ***p<0.001).
708
709 **Figure 5—figure supplement 1 | HPV-positive HNSCC express lower levels of**
710 **differentiation genes.** RNA-seq data from TCGA were accessed through cBioPortal. Violin plots
711 display the distribution in $\log_2$ mRNA expression of differentiation markers (A) KRT1, (B) KRT10,

712 and (C) IVL, and the canonical YAP1/TAZ targets (D) CTGF and (E) CYR61. Statistical
713 significance was determined by Mann-Whitney nonparametric test. (**p<0.01, ***p<0.001,
714 ****p<0.0001).
715
716 **Figure 7—figure supplement 1 | PTPN14 degradation by HPV E7 promotes basal cell**
717 **retention.** (A-B) GFP-labeled HFK were transduced with YAP1 WT, YAP1 S127A, or YAP1 S94A
718 under the control of a doxycycline inducible promoter. (A) GFP expression was confirmed by
719 fluorescence microscopy. Scale bar = 100 μm. (B) Total RNA was purified from monolayer cells
720 +/- treatment with 1 μg/mL doxycycline for 72h. qRT-PCR was used to assess gene expression
721 of YAP1 and CTGF. (C-D) GFP-labeled HFK were transduced with retroviral vectors encoding
722 HPV18 WT, HPV18 ΔDLLC, HPV18 E7 R84S, or the empty vector control (EV). (C) GFP
723 expression was confirmed by fluorescence microscopy. Scale bar = 100 μm. (D) Cell lysates were
724 subjected to SDS/PAGE/Western analysis and probed with antibodies to PTPN14, RB1, and
725 Actin. (E-F) GFP-labeled HFK were transduced with LentiCRISPR v2 sgNT-1, sgPTPN14-3, or
726 sgPTPN14-4 vectors. (E) GFP expression was confirmed by fluorescence microscopy. Scale bar
727 = 100 μm (F) Cell lysates were subjected to SDS/PAGE/Western analysis and probed with
728 antibodies to PTPN14 and Actin.
729
730 **Figure 7—figure supplement 2 | HPV18 E7 can promote basal cell retention in the absence**
731 **of RB1 binding.** Organotypic cultures were grown from GFP-labeled cells mixed with unmodified
732 HFK. GFP-labeled HFK were transduced with HPV18 E7 ΔDLLC or the empty vector (EV). GFP-
733 labeled cells were mixed 1:50 into unmodified HFK. (A) FFPE sections were stained for GFP
734 (green), IVL (grey), and Hoechst (blue). Scale bar = 100 μm (B) Quantification of the percentage
735 of GFP+ cells found in the basal layer. Graphs display the mean ± SD and each individual data
736 point (independent cultures). Statistical significance was determined by t-test. (**p<0.01).
737

References

Alzahrani F, Clattenburg L, Muruganandan S, Bullock M, MacIsaac K, Wigerius M, Williams BA, Graham MER, Rigby MH, Trites JRB, Taylor SM, Sinal CJ, Fawcett JP, Hart RD. 2017. The Hippo component YAP localizes in the nucleus of human papilloma virus positive oropharyngeal squamous cell carcinoma. *Journal of Otolaryngology - Head and Neck Surgery* **46**. doi:10.1186/s40463-017-0187-1

Balsitis S, Dick F, Dyson N, Lambert PF. 2006. Critical Roles for Non-pRb Targets of Human Papillomavirus Type 16 E7 in Cervical Carcinogenesis. *Cancer Res* **66**:9393–400. doi:10.1158/0008-5472.CAN-06-0984

Balsitis S, Dick F, Lee D, Farrell L, Hyde RK, Griep AE, Dyson N, Lambert PF. 2005. Examination of the pRb-Dependent and pRb-Independent Functions of E7 In Vivo. *Journal of Virology* **79**:11392–11402. doi:10.1128/jvi.79.17.11392-11402.2005

Banks L, Edmonds C, Vousden KH. 1990. Ability of the HPV16 E7 protein to bind RB and induce DNA synthesis is not sufficient for efficient transforming activity in NIH3T3 cells. *Oncogene* **5**:1383–9.

Beverdam A, Claxton C, Zhang X, James G, Harvey KF, Key B. 2013. Yap Controls Stem/Progenitor Cell Proliferation in the Mouse Postnatal Epidermis. *Journal of Investigative Dermatology* **133**:1497–1505. doi:10.1038/JID.2012.430

Bonilla X, Parmentier L, King B, Bezrukov F, Kaya G, Zoete V, Seplyarskiy VB, Sharpe HJ, McKee T, Letourneau A, Ribaux PG, Popadin K, Basset-Seguin N, Chaabene R ben, Santoni FA, Andrianova MA, Guipponi M, Garieri M, Verdan C, Grosdemange K, Sumara O, Eilers M, Aifantis I, Michielin O, de Sauvage FJ, Antonarakis SE, Nikolaev SI. 2016. Genomic analysis identifies new drivers and progression pathways in skin basal cell carcinoma. *Nature Genetics* **48**:398–406. doi:10.1038/ng.3525

Campeau E, Ruhl VE, Rodier F, Smith CL, Rahmberg BL, Fuss JO, Campisi J, Yaswen P, Cooper PK, Kaufman PD. 2009. A Versatile Viral System for Expression and Depletion of Proteins in Mammalian Cells. *PLOS ONE* **4**:e6529. doi:10.1371/JOURNAL.PONE.0006529

Cerami E, Gao J, Dogrusoz U, Gross BE, Sumer SO, Aksoy BA, Jacobsen A, Byrne CJ, Heuer ML, Larsson E, Antipin Y, Reva B, Goldberg AP, Sander C, Schultz N. 2012. The cBio Cancer Genomics Portal: An Open Platform for Exploring Multidimensional Cancer Genomics Data. *Cancer Discovery* **2**:401–404. doi:10.1158/2159-8290.CD-12-0095

Chakravarthy A, Henderson S, Thirdborough SM, Ottensmeier CH, Su X, Lechner M, Feber A, Thomas GJ, Fenton TR. 2016. Human Papillomavirus Drives Tumor Development Throughout the Head and Neck: Improved Prognosis Is Associated With an Immune Response Largely Restricted to the Oropharynx. *https://doi.org/101200/JCO2016682955* **34**:4132–4141. doi:10.1200/JCO.2016.68.2955

Ciccolini F, di Pasquale G, Carlotti F, Crawford L, Tommasino M. 1994. Functional studies of E7 proteins from different HPV types. *Oncogene* **9**:2633–8.

776 Collins AS, Nakahara T, Do A, Lambert PF. 2005. Interactions with pocket proteins contribute to
777 the role of human papillomavirus type 16 E7 in the papillomavirus life cycle. *J Virol*
778 **79**:14769–80. doi:10.1128/JVI.79.23.14769-14780.2005

779 Day PM, Schelhaas M. 2014. Concepts of papillomavirus entry into host cells. *Current Opinion*
780 *in Virology* **4**:24–31. doi:10.1016/J.COVIRO.2013.11.002

781 de Martel C, Georges D, Bray F, Ferlay J, Clifford GM. 2020. Global burden of cancer
782 attributable to infections in 2018: a worldwide incidence analysis. *The Lancet Global Health*
783 **8**:e180–e190. doi:10.1016/S2214-109X(19)30488-7/ATTACHMENT/BC543EDD-015D-
784 48D3-A3FB-6DFCF0BCDE7F/MMC1.PDF

785 de Martel C, Plummer M, Vignat J, Franceschi S. 2017. Worldwide burden of cancer attributable
786 to HPV by site, country and HPV type. *International Journal of Cancer* **141**:664–670.
787 doi:10.1002/ijc.30716

788 Dickson MA, Hahn WC, Ino Y, Ronfard V, Wu JY, Weinberg RA, Louis DN, Li FP, Rheinwald
789 JG. 2000. Human Keratinocytes That Express hTERT and Also Bypass a p16INK4a-
790 Enforced Mechanism That Limits Life Span Become Immortal yet Retain Normal Growth
791 and Differentiation Characteristics. *Molecular and Cellular Biology* **20**:1436–1447.
792 doi:10.1128/mcb.20.4.1436-1447.2000

793 Doorbar J, Egawa N, Griffin H, Kranjec C, Murakami I. 2015. Human papillomavirus molecular
794 biology and disease association. *Reviews in Medical Virology* **25**:2–23.
795 doi:10.1002/rmv.1822

796 Duperret EK, Dahal A, Ridky TW. 2015. Focal-adhesion-independent integrin-av regulation of
797 FAK and c-Myc is necessary for 3D skin formation and tumor invasion. *Journal of Cell*
798 *Science* **128**:3997–4013. doi:10.1242/jcs.175539

799 Egawa N, Nakahara T, Ohno S -i., Narisawa-Saito M, Yugawa T, Fujita M, Yamato K, Natori Y,
800 Kiyono T. 2012. The E1 Protein of Human Papillomavirus Type 16 Is Dispensable for
801 Maintenance Replication of the Viral Genome. *Journal of Virology*. doi:10.1128/JVI.06450-
802 11

803 Egolf S, Aubert Y, Doepner M, Anderson A, Maldonado-Lopez A, Pacella G, Lee J, Ko EK, Zou
804 J, Lan Y, Simpson CL, Ridky T, Capell BC. 2019. LSD1 Inhibition Promotes Epithelial
805 Differentiation through Derepression of Fate-Determining Transcription Factors. *Cell*
806 *Reports* **28**:1981-1992.e7. doi:10.1016/j.celrep.2019.07.058

807 Elbediwy A, Thompson BJ. 2018. Evolution of mechanotransduction via YAP/TAZ in animal
808 epithelia. *Current Opinion in Cell Biology*. doi:10.1016/j.ceb.2018.02.003

809 Elbediwy A, Vincent-Mistiaen ZI, Spencer-Dene B, Stone RK, Boeing S, Wculek SK, Cordero J,
810 Tan EH, Ridgway R, Brunton VG, Sahai E, Gerhardt H, Behrens A, Malanchi I, Sansom
811 OJ, Thompson BJ. 2016. Integrin signalling regulates YAP and TAZ to control skin
812 homeostasis. *Development (Cambridge, England)* **143**:1674–87. doi:10.1242/dev.133728

813 Facompre ND, Rajagopalan P, Sahu V, Pearson AT, Montone KT, James CD, Gleber-Netto FO,
814 Weinstein GS, Jalaly J, Lin A, Rustgi AK, Nakagawa H, Califano JA, Pickering CR, White
815 EA, Windle BE, Morgan IM, Cohen RB, Gimotty PA, Basu D. 2020. Identifying predictors of
816 HPV-related head and neck squamous cell carcinoma progression and survival through

817 patient-derived models. *International Journal of Cancer* **147**:3236–3249.
818 doi:10.1002/IJC.33125

819 Fehrmann F, Laimins LA. 2005. Human Papillomavirus Type 31 Life Cycle Methods for
820 Studying Using Tissue Culture Models. *Methods in Molecular Biology* **292**:317–330.

821 Flores ER, Allen-Hoffmann BL, Lee D, Lambert PF. 2000. The human papillomavirus type 16 E7
822 oncogene is required for the productive stage of the viral life cycle. *Journal of virology*
823 **74**:6622–31. doi:10.1128/JVI.74.14.6622-6631.2000

824 Galligan JT, Martinez-Noël G, Arndt V, Hayes S, Chittenden TW, Harper JW, Howley PM. 2014.
825 Proteomic Analysis and Identification of Cellular Interactors of the Giant Ubiquitin Ligase
826 HERC2. *Journal of Proteome Research* **14**:953–966. doi:10.1021/PR501005V

827 Gao J, Aksoy BA, Dogrusoz U, Dresdner G, Gross B, Sumer SO, Sun Y, Jacobsen A, Sinha R,
828 Larsson E, Cerami E, Sander C, Schultz N. 2013. Integrative Analysis of Complex Cancer
829 Genomics and Clinical Profiles Using the cBioPortal. *Science Signaling* **6**:1–1.
830 doi:10.1126/SCISIGNAL.2004088

831 Gillison ML, Chaturvedi AK, Anderson WF, Fakhry C. 2015. Epidemiology of Human
832 Papillomavirus-Positive Head and Neck Squamous Cell Carcinoma. *J Clin Oncol* **33**:3235–
833 3242. doi:10.1200/JCO.2015.61.6995

834 Graham S v. 2017. The human papillomavirus replication cycle, and its links to cancer
835 progression: a comprehensive review. *Clinical Science* **131**:2201–2221.
836 doi:10.1042/CS20160786

837 Halbert CL, Demers GW, Galloway DA. 1991. The E7 gene of human papillomavirus type 16 is
838 sufficient for immortalization of human epithelial cells. *Journal of virology* **65**:473–8.

839 Hatterschide J, Bohidar AE, Grace M, Nulton TJ, Kim HW, Windle B, Morgan IM, Munger K,
840 White EA. 2019. PTPN14 degradation by high-risk human papillomavirus E7 limits
841 keratinocyte differentiation and contributes to HPV-mediated oncogenesis. *Proceedings of*
842 *the National Academy of Sciences of the United States of America* **116**:7033–7042.
843 doi:10.1073/pnas.1819534116

844 Hatterschide J, Brantly AC, Grace M, Munger K, White EA. 2020. A Conserved Amino Acid in
845 the C Terminus of Human Papillomavirus E7 Mediates Binding to PTPN14 and Repression
846 of Epithelial Differentiation. *Journal of Virology* **94**. doi:10.1128/jvi.01024-20

847 He C, Lv X, Huang C, Angeletti PC, Hua G, Dong J, Zhou J, Wang Z, Ma B, Chen X, Lambert
848 PF, Rueda BR, Davis JS, Wang C. 2019. A Human Papillomavirus-Independent Cervical
849 Cancer Animal Model Reveals Unconventional Mechanisms of Cervical Carcinogenesis.
850 *Cell Reports* **26**. doi:10.1016/j.celrep.2019.02.004

851 He C, Mao D, Hua G, Lv X, Chen X, Angeletti PC, Dong J, Remmenga SW, Rodabaugh KJ,
852 Zhou J, Lambert PF, Yang P, Davis JS, Wang C. 2015. The Hippo/YAP pathway interacts
853 with EGFR signaling and HPV oncoproteins to regulate cervical cancer progression. *EMBO*
854 *molecular medicine* **7**:1426–49. doi:10.15252/emmm.201404976

855 Heck D v, Yee CL, Howley PM, Münger K. 1992. Efficiency of binding the retinoblastoma protein
856 correlates with the transforming capacity of the E7 oncoproteins of the human

papillomaviruses. *Proceedings of the National Academy of Sciences of the United States of America* **89**:4442–6. doi:10.1073/PNAS.89.10.4442

Helt A-MA-M, Galloway DA. 2002. Destabilization of the Retinoblastoma Tumor Suppressor by Human Papillomavirus Type 16 E7 Is Not Sufficient To Overcome Cell Cycle Arrest in Human Keratinocytes. *JOURNAL OF VIROLOGY* **75**:6737–6747. doi:10.1128/JVI.75.15.6737-6747.2001

Heng BC, Zhang X, Aubel D, Bai Y, Li X, Wei Y, Fussenegger M, Deng X. 2020. Role of YAP/TAZ in Cell Lineage Fate Determination and Related Signaling Pathways. *Frontiers in Cell and Developmental Biology* **0**:735. doi:10.3389/FCELL.2020.00735

Hicks-Berthet J, Ning B, Federico A, Tilston-Lunel A, Matschulat A, Ai X, Lenburg ME, Beane J, Monti S, Varelas X. 2021. Yap/Taz inhibit goblet cell fate to maintain lung epithelial homeostasis. *Cell Reports* **36**. doi:10.1016/J.CELREP.2021.109347

Huh KW, DeMasi J, Ogawa H, Nakatani Y, Howley PM, Münger K. 2005. Association of the human papillomavirus type 16 E7 oncoprotein with the 600-kDa retinoblastoma protein-associated factor, p600. *Proceedings of the National Academy of Sciences of the United States of America* **102**:11492–11497. doi:10.1073/pnas.0505337102

Hwang JH, Pores Fernando AT, Faure N, Andrabi S, Adelmant G, Hahn WC, Marto JA, Schaffhausen BS, Roberts TM. 2014. Polyomavirus small T antigen interacts with yes-associated protein to regulate cell survival and differentiation. *Journal of virology* **88**:12055–64. doi:10.1128/JVI.01399-14

Ibaraki T, Satake M, Kurai N, Ichijo M, Ito Y. 1993. Transacting activities of the E7 genes of several types of human papillomavirus. *Virus Genes* **7**:187–196. doi:10.1007/BF01702398

Jewers RJ, Hildebrandt P, Ludlow JW, Kell B, McCance DJ. 1992. Regions of human papillomavirus type 16 E7 oncoprotein required for immortalization of human keratinocytes. *Journal of virology* **66**:1329–35.

Kho E-Y, Wang H-K, Banerjee NS, Broker TR, Chow LT. 2013. HPV-18 E6 mutants reveal p53 modulation of viral DNA amplification in organotypic cultures. *Proceedings of the National Academy of Sciences* **110**:7542–7549. doi:10.1073/PNAS.1304855110

Knight JF, Sung VYC, Kuzmin E, Couzens AL, de Verteuil DA, Ratcliffe CDH, Coelho PP, Johnson RM, Samavarchi-Tehrani P, Gruosso T, Smith HW, Lee W, Saleh SM, Zuo D, Zhao H, Guiot MC, Davis RR, Gregg JP, Moraes C, Gingras AC, Park M. 2018. KIBRA (WWC1) Is a Metastasis Suppressor Gene Affected by Chromosome 5q Loss in Triple-Negative Breast Cancer. *Cell Reports* **22**:3191–3205. doi:10.1016/j.celrep.2018.02.095

Knox KK, Carrigan DR. 1992. In Vitro Suppression of Bone Marrow Progenitor Cell Differentiation by Human Herpesvirus 6 Infection. *The Journal of Infectious Diseases* **165**:925–928. doi:10.1093/INFDIS/165.5.925

Koshiol J, Lindsay L, Pimenta JM, Poole C, Jenkins D, Smith JS. 2008. Persistent human papillomavirus infection and cervical neoplasia: A systematic review and meta-analysis. *American Journal of Epidemiology*. doi:10.1093/aje/kwn036

Kranjec C, Holleywood C, Libert D, Griffin H, Mahmood R, Isaacson E, Doorbar J. 2017. Modulation of basal cell fate during productive and transforming HPV-16 infection is mediated by progressive E6-driven depletion of Notch. *The Journal of Pathology* **242**:448–462. doi:10.1002/path.4917

Lawrence MS, Sougnez C, Lichtenstein L, Cibulskis K, Lander E, Gabriel SB, Getz G, Ally A, Balasundaram M, Birol I, Bowlby R, Brooks D, Butterfield YSN, Carlsen R, Cheng D, Chu A, Dhalla N, Guin R, Holt RA, Jones SJM, Lee D, Li HI, Marra MA, Mayo M, Moore RA, Mungall AJ, Robertson AG, Schein JE, Sipahimalani P, Tam A, Thiessen N, Wong T, Protopopov A, Santoso N, Lee S, Parfenov M, Zhang Jianhua, Mahadeshwar HS, Tang J, Ren X, Seth S, Haseley P, Zeng D, Yang Lixing, Xu AW, Song X, Pantazi A, Bristow CA, Hadjipanayis A, Seidman J, Chin L, Park PJ, Kucherlapati R, Akbani R, Casasent T, Liu W, Lu Y, Mills G, Motter T, Weinstein J, Diao L, Wang J, Hong Fan Y, Liu J, Wang K, Auman JT, Balu S, Bodenheimer T, Buda E, Hayes DN, Hoadley KA, Hoyle AP, Jefferys SR, Jones CD, Kimes PK, Liu Yufeng, Marron JS, Meng S, Mieczkowski PA, Mose LE, Parker JS, Perou CM, Prins JF, Roach J, Shi Y, Simons J v., Singh D, Soloway MG, Tan D, Veluvolu U, Walter V, Waring S, Wilkerson MD, Wu J, Zhao N, Cherniack AD, Hammerman PS, Tward AD, Pedamallu CS, Saksena G, Jung J, Ojesina AI, Carter SL, Zack TI, Schumacher SE, Beroukhim R, Freeman SS, Meyerson M, Cho J, Noble MS, DiCara D, Zhang H, Heiman DI, Gehlenborg N, Voet D, Lin P, Frazer S, Stojanov P, Liu Yingchun, Zou L, Kim J, Muzny D, Doddapaneni HV, Kovar C, Reid J, Morton D, Han Y, Hale W, Chao H, Chang K, Drummond JA, Gibbs RA, Kakkar N, Wheeler D, Xi L, Ciriello G, Ladanyi M, Lee W, Ramirez R, Sander C, Shen R, Sinha R, Weinhold N, Taylor BS, Aksoy BA, Dresdner G, Gao J, Gross B, Jacobsen A, Reva B, Schultz N, Sumer SO, Sun Y, Chan TA, Morris LG, Stuart J, Benz S, Ng S, Benz C, Yau C, Baylin SB, Cope L, Danilova L, Herman JG, Bootwalla M, Maglinte DT, Laird PW, Triche T, Weisenberger DJ, van den Berg DJ, Agrawal N, Bishop J, Boutros PC, Bruce JP, Byers LA, Califano J, Carey TE, Chen Z, Cheng H, Chiosea SI, Cohen E, Diergaarde B, Egloff AM, El-Naggar AK, Ferris RL, Frederick MJ, Grandis JR, Guo Y, Haddad RI, Harris T, Hui ABY, Lee JJ, Lippman SM, Liu FF, McHugh JB, Myers J, Ng PKS, Perez-Ordonez B, Pickering CR, Prystowsky M, Romkes M, Saleh AD, Sartor MA, Seethala R, Seiwert TY, Si H, van Waes C, Waggott DM, Wiznerowicz M, Yarbrough WG, Zhang Jiexin, Zuo Z, Burnett K, Crain D, Gardner J, Lau K, Mallery D, Morris S, Paulauskis J, Penny R, Shelton C, Shelton T, Sherman M, Yena P, Black AD, Bowen J, Frick J, Gastier-Foster JM, Harper HA, Leraas K, Lichtenberg TM, Ramirez NC, Wise L, Zmuda E, Baboud J, Jensen MA, Kahn AB, Pihl TD, Pot DA, Srinivasan D, Walton JS, Wan Y, Burton RA, Davidsen T, Demchok JA, Eley G, Ferguson ML, Mills Shaw KR, Ozenberger BA, Sheth M, Sofia HJ, Tarnuzzer R, Wang Z, Yang Liming, Zenklusen JC, Saller C, Tarvin K, Chen C, Bollag R, Weinberger P, Golusiński W, Golusiński P, Ibbs M, Korski K, Mackiewicz A, Suchorska W, Szybiak B, Curley E, Beard C, Mitchell C, Sandusky G, Ahn J, Khan Z, Irish J, Waldron J, William WN, Egea S, Gomez-Fernandez C, Herbert L, Bradford CR, Chepeha DB, Haddad AS, Jones TR, Komarck CM, Malakh M, Moyer JS, Nguyen A, Peterson LA, Prince ME, Rozek LS, Taylor EG, Walline HM, Wolf GT, Boice L, Chera BS, Funkhouser WK, Gulley ML, Hackman TG, Hayward MC, Huang M, Rathmell WK, Salazar AH, Shockley WW, Shores CG, Thorne L, Weissler MC, Wrenn S, Zanation AM, Brown BT, Pham M. 2015. Comprehensive genomic characterization of head and neck squamous cell carcinomas. *Nature 2015 517:7536* **517**:576–582. doi:10.1038/nature14129

Lewis JS, Beadle B, Bishop JA, Chernock RD, Colasacco C, Lacchetti C, Moncur JT, Rocco JW, Schwartz MR, Seethala RR, Thomas NE, Westra WH, Faquin WC. 2018. Human Papillomavirus Testing in Head and Neck Carcinomas: Guideline From the College of American Pathologists. *Archives of Pathology & Laboratory Medicine* **142**:559–597. doi:10.5858/ARPA.2017-0286-CP

Liu G, Yu F-X, Kim YC, Meng Z, Naipauer J, Looney DJ, Liu X, Gutkind JS, Mesri EA, Guan K-L. 2014. Kaposi sarcoma-associated herpesvirus promotes tumorigenesis by modulating the Hippo pathway. *Oncogene 2015 34:27* **34**:3536–3546. doi:10.1038/onc.2014.281

Liu K, Du S, Gao P, Zheng J. 2019. Verteporfin suppresses the proliferation, epithelial-mesenchymal transition and stemness of head and neck squamous carcinoma cells via inhibiting YAP1. *Journal of Cancer* **10**:4196–4207. doi:10.7150/jca.34145

Liu P, Zhang H, Liang X, Ma H, Luan F, Wang B, Bai F, Gao L, Ma C. 2015. HBV preS2 promotes the expression of TAZ via miRNA-338-3p to enhance the tumorigenesis of hepatocellular carcinoma. *Oncotarget* **6**:29048. doi:10.18632/ONCOTARGET.4804

McBride AA. 2021. Human papillomaviruses: diversity, infection and host interactions. *Nature Reviews Microbiology*. doi:10.1038/s41579-021-00617-5

McBride AA. 2017. Mechanisms and strategies of papillomavirus replication. *Biological Chemistry* **398**:919–927. doi:10.1515/hsz-2017-0113

McLaughlin-Drubin ME, Bromberg-White JL, Meyers C. 2005. The role of the human papillomavirus type 18 E7 oncoprotein during the complete viral life cycle. *Virology* **338**:61–68. doi:10.1016/j.virol.2005.04.036

Mello SS, Valente LJ, Raj N, Seoane JA, Flowers BM, McClendon J, Bieging-Rolett KT, Lee J, Ivanochko D, Kozak MM, Chang DT, Longacre TA, Koong AC, Arrowsmith CH, Kim SK, Vogel H, Wood LD, Hruban RH, Curtis C, Attardi LD. 2017. A p53 Super-tumor Suppressor Reveals a Tumor Suppressive p53-Ptpn14-Yap Axis in Pancreatic Cancer. *Cancer Cell* **32**:460-473.e6. doi:10.1016/j.ccell.2017.09.007

Mendelsohn AH, Lai CK, Shintaku IP, Elashoff DA, Dubinett SM, Abemayor E, st. John MA. 2010. Histopathologic findings of HPV and p16 positive HNSCC. *The Laryngoscope* **120**:1788–1794. doi:10.1002/lary.21044

Mirabello L, Yeager M, Yu K, Clifford GM, Xiao Y, Zhu B, Cullen M, Boland JF, Wentzensen N, Nelson CW, Raine-Bennett T, Chen Z, Bass S, Song L, Yang Q, Steinberg M, Burdett L, Dean M, Roberson D, Mitchell J, Lorey T, Franceschi S, Castle PE, Walker J, Zuna R, Kreimer AR, Beachler DC, Hildesheim A, Gonzalez P, Porras C, Burk RD, Schiffman M. 2017. HPV16 E7 Genetic Conservation Is Critical to Carcinogenesis. *Cell* **170**:1164-1174.e6.

Morgan EL, Patterson MR, Ryder EL, Lee SY, Wasson CW, Harper KL, Li Y, Griffin S, Blair GE, Whitehouse A, Macdonald A. 2020. MicroRNA-18a targeting of the STK4/MST1 tumour suppressor is necessary for transformation in HPV positive cervical cancer. *PLOS Pathogens* **16**:e1008624. doi:10.1371/journal.ppat.1008624

Moroishi T, Hansen CG, Guan K-L. 2015. The emerging roles of YAP and TAZ in cancer. *Nature Reviews Cancer* **15**:73–79. doi:10.1038/nrc3876

983 Münger K, Werness BA, Dyson N, Phelps WC, Harlow E, Howley PM. 1989. Complex formation
984 of human papillomavirus E7 proteins with the retinoblastoma tumor suppressor gene
985 product. *The EMBO Journal* **8**:4099–4105. doi:10.1002/j.1460-2075.1989.tb08594.x

986 Nguyen HT, Hong X, Tan S, Chen Q, Chan L, Fivaz M, Cohen SM, Voorhoeve PM. 2014. Viral
987 Small T Oncoproteins Transform Cells by Alleviating Hippo-Pathway-Mediated Inhibition of
988 the YAP Proto-oncogene. *Cell Reports* **8**:707–713. doi:10.1016/J.CELREP.2014.06.062

989 Niiya H, Lei J, Guo Y, Azuma T, Yakushijin Y, Sakai I, Hato T, Tohyama M, Hashimoto K,
990 Yasukawa M. 2006. Human herpesvirus 6 impairs differentiation of monocytes to dendritic
991 cells. *Experimental Hematology* **34**:642–653. doi:10.1016/J.EXPHEM.2006.02.001

992 Nishio M, To Y, Maehama T, Aono Y, Otani J, Hikasa H, Kitagawa A, Mimori K, Sasaki T,
993 Nishina H, Toyokuni S, Lydon JP, Nakao K, Mak TW, Kiyono T, Katabuchi H, Tashiro H,
994 Suzuki A. 2020. Endogenous YAP1 activation drives immediate onset of cervical
995 carcinoma in situ in mice. *Cancer Science* **111**:3576. doi:10.1111/CAS.14581

996 Olafsdottir T, Stacey SN, Sveinbjornsson G, Thorleifsson G, Norland K, Sigurgeirsson B,
997 Thorisdottir K, Kristjansson AK, Tryggvadottir L, Sarin KY, Benediktsson R, Jonasson JG,
998 Sigurdsson A, Jonasdottir A, Kristmundsdottir S, Jonsson H, Gylfason A, Oddsson A,
999 Fridriksdottir R, Gudjonsson SA, Zink F, Lund SH, Rognvaldsson S, Melsted P,
1000 Steinthorsdottir V, Gudmundsson J, Mikaelsdottir E, Olason PI, Stefansdottir L, Eggertsson
1001 HP, Halldorsson B v., Thorsteinsdottir U, Agustsson TT, Olafsson K, Olafsson JH, Sulem
1002 P, Rafnar T, Gudbjartsson DF, Stefansson K. 2021. Loss-of-Function Variants in the
1003 Tumor-Suppressor Gene PTPN14 Confer Increased Cancer Risk. *Cancer Research*
1004 **81**:1954–1964. doi:10.1158/0008-5472.CAN-20-3065

1005 Olmedo-Nieva L, Muñoz-Bello JO, Manzo-Merino J, Lizano M. 2020. New insights in Hippo
1006 signalling alteration in human papillomavirus-related cancers. *Cellular Signalling* 109815.
1007 doi:10.1016/j.cellsig.2020.109815

1008 Omori H, Nishio M, Masuda M, Miyachi Y, Ueda F, Nakano T, Sato K, Mimori K, Taguchi K,
1009 Hikasa H, Nishina H, Tashiro H, Kiyono T, Mak TW, Nakao K, Nakagawa T, Maehama T,
1010 Suzuki A. 2020. YAP1 is a potent driver of the onset and progression of oral squamous cell
1011 carcinoma. *Science Advances* **6**:eaay3324. doi:10.1126/sciadv.aay3324

1012 Onnis A, Navari M, Antonicelli G, Morettini F, Mannucci S, de Falco G, Vigorito E, Leoncini L.
1013 2012. Epstein-Barr nuclear antigen 1 induces expression of the cellular microRNA hsa-
1014 miR-127 and impairing B-cell differentiation in EBV-infected memory B cells. New insights
1015 into the pathogenesis of Burkitt lymphoma. *Blood Cancer Journal 2012 2:8* **2**:e84–e84.
1016 doi:10.1038/bcj.2012.29

1017 Pai SI, Westra WH. 2009. Molecular Pathology of Head and Neck Cancer: Implications for
1018 Diagnosis, Prognosis, and Treatment. *Annual Review of Pathology: Mechanisms of*
1019 *Disease* **4**:49–70. doi:10.1146/annurev.pathol.4.110807.092158

1020 Parish JL, Bean AM, Park RB, Androphy EJ. 2006. ChlR1 Is Required for Loading
1021 Papillomavirus E2 onto Mitotic Chromosomes and Viral Genome Maintenance. *Molecular*
1022 *Cell* **24**:867–876. doi:10.1016/j.molcel.2006.11.005

1023 Perez CA, Ott J, Mays DJ, Pietenpol JA. 2007. p63 consensus DNA-binding site: identification,
1024 analysis and application into a p63MH algorithm. *Oncogene* **26**:7363–7370.
1025 doi:10.1038/sj.onc.1210561

1026 Phelps WC, Münger K, Yee CL, Barnes JA, Howley PM. 1992. Structure-function analysis of the
1027 human papillomavirus type 16 E7 oncoprotein. *Journal of Virology* **66**:2418–2427.
1028 doi:10.1128/jvi.66.4.2418-2427.1992

1029 Poernbacher I, Baumgartner R, Marada SK, Edwards K, Stocker H. 2012. Drosophila Pez acts
1030 in Hippo signaling to restrict intestinal stem cell proliferation. *Current biology : CB* **22**:389–
1031 96. doi:10.1016/j.cub.2012.01.019

1032 Pyeon D, Pearce SM, Lank SM, Ahlquist P, Lambert PF. 2009. Establishment of human
1033 papillomavirus infection requires cell cycle progression. *PLoS Pathogens* **5**:e1000318.
1034 doi:10.1371/journal.ppat.1000318

1035 Radley D, Saah A, Stanley M. 2016. Persistent infection with human papillomavirus 16 or 18 is
1036 strongly linked with high-grade cervical disease. *Human Vaccines & Immunotherapeutics*
1037 **12**:768–772. doi:10.1080/21645515.2015.1088616

1038 Roberts JN, Buck CB, Thompson CD, Kines R, Bernardo M, Choyke PL, Lowy DR, Schiller JT.
1039 2007. Genital transmission of HPV in a mouse model is potentiated by nonoxynol-9 and
1040 inhibited by carrageenan. *Nature Medicine 2007 13:7* **13**:857–861. doi:10.1038/nm1598

1041 Roh M, Song C, Kim J, Abdulkadir SA. 2005. Chromosomal Instability Induced by Pim-1 Is
1042 Passage-dependent and Associated with Dysregulation of Cyclin B1 *. *Journal of Biological*
1043 *Chemistry* **280**:40568–40577. doi:10.1074/JBC.M509369200

1044 Romeo MA, Gilardini Montani MS, Falcinelli L, Gaeta A, Nazzari C, Faggioni A, Cirone M. 2019.
1045 HHV-6B reduces autophagy and induces ER stress in primary monocytes impairing their
1046 survival and differentiation into dendritic cells. *Virus Research* **273**:197757.
1047 doi:10.1016/J.VIRUSRES.2019.197757

1048 Rositch AF, Koshiol J, Hudgens MG, Razzaghi H, Backes DM, Pimenta JM, Franco EL, Poole
1049 C, Smith JS. 2013. Patterns of persistent genital human papillomavirus infection among
1050 women worldwide: A literature review and meta-analysis. *International Journal of Cancer*
1051 **133**:1271–1285. doi:10.1002/ijc.27828

1052 Sanchez-Vega F, Mina M, Armenia J, Chatila WK, Luna A, La KC, Dimitriadoy S, Liu DL,
1053 Kantheti HS, Saghafinia S, Chakravarty D, Daian F, Gao Q, Bailey MH, Liang WW, Foltz
1054 SM, Shmulevich I, Ding L, Heins Z, Ochoa A, Gross B, Gao J, Zhang Hongxin, Kundra R,
1055 Kandoth C, Bahceci I, Dervishi L, Dogrusoz U, Zhou W, Shen H, Laird PW, Way GP,
1056 Greene CS, Liang H, Xiao Y, Wang C, Iavarone A, Berger AH, Bivona TG, Lazar AJ,
1057 Hammer GD, Giordano T, Kwong LN, McArthur G, Huang C, Tward AD, Frederick MJ,
1058 McCormick F, Meyerson M, Caesar-Johnson SJ, Demchok JA, Felau I, Kasapi M,
1059 Ferguson ML, Hutter CM, Sofia HJ, Tarnuzzer R, Wang Z, Yang L, Zenklusen JC, Zhang J
1060 (Julia), Chudamani S, Liu J, Lolla L, Naresh R, Pihl T, Sun Q, Wan Y, Wu Y, Cho J,
1061 DeFreitas T, Frazer S, Gehlenborg N, Getz G, Heiman DI, Kim J, Lawrence MS, Lin P,
1062 Meier S, Noble MS, Saksena G, Voet D, Zhang Hailei, Bernard B, Chambwe N, Dhankani
1063 V, Knijnenburg T, Kramer R, Leinonen K, Liu Y, Miller M, Reynolds S, Shmulevich I,
1064 Thorsson V, Zhang W, Akbani R, Broom BM, Hegde AM, Ju Z, Kanchi RS, Korkut A, Li J,

Liang H, Ling S, Liu W, Lu Y, Mills GB, Ng KS, Rao A, Ryan M, Wang Jing, Weinstein JN, Zhang J, Abeshouse A, Armenia J, Chakravarty D, Chatila WK, de Bruijn I, Gross BE, Heins ZJ, Kundra R, La K, Ladanyi M, Luna A, Nissan MG, Ochoa A, Phillips SM, Reznik E, Sanchez-Vega F, Sander C, Schultz N, Sheridan R, Sumer SO, Sun Y, Taylor BS, Wang Jioajiao, Zhang Hongxin, Anur P, Peto M, Spellman P, Benz C, Stuart JM, Wong CK, Yau C, Hayes DN, Parker JS, Wilkerson MD, Ally A, Balasundaram M, Bowlby R, Brooks D, Carlsen R, Chuah E, Dhalla N, Holt R, Jones SJM, Kasaian K, Lee D, Ma Y, Marra MA, Mayo M, Moore RA, Mungall AJ, Mungall K, Robertson AG, Sadeghi S, Schein JE, Sipahimalani P, Tam A, Thiessen N, Tse K, Wong T, Berger AC, Beroukhim R, Cherniack AD, Cibulskis C, Gabriel SB, Gao GF, Ha G, Meyerson M, Schumacher SE, Shih J, Kucherlapati MH, Kucherlapati RS, Baylin S, Cope L, Danilova L, Bootwalla MS, Lai PH, Maglinte DT, van den Berg DJ, Weisenberger DJ, Auman JT, Balu S, Bodenheimer T, Fan C, Hoadley KA, Hoyle AP, Jefferys SR, Jones CD, Meng S, Mieczkowski PA, Mose LE, Perou AH, Perou CM, Roach J, Shi Y, Simons J v., Skelly T, Soloway MG, Tan D, Veluvolu U, Fan H, Hinoue T, Laird PW, Shen H, Zhou W, Bellair M, Chang K, Covington K, Creighton CJ, Dinh H, Doddapaneni HV, Donehower LA, Drummond J, Gibbs RA, Glenn R, Hale W, Han Y, Hu J, Korchina V, Lee S, Lewis L, Li W, Liu X, Morgan M, Morton D, Muzny D, Santibanez J, Sheth M, Shinbrot E, Wang L, Wang M, Wheeler DA, Xi L, Zhao F, Hess J, Appelbaum EL, Bailey M, Cordes MG, Ding L, Fronick CC, Fulton LA, Fulton RS, Kandoth C, Mardis ER, McLellan MD, Miller CA, Schmidt HK, Wilson RK, Crain D, Curley E, Gardner J, Lau K, Mallery D, Morris S, Paulauskis J, Penny R, Shelton C, Shelton T, Sherman M, Thompson E, Yena P, Bowen J, Gastier-Foster JM, Gerken M, Leraas KM, Lichtenberg TM, Ramirez NC, Wise L, Zmuda E, Corcoran N, Costello T, Hovens C, Carvalho AL, de Carvalho AC, Fregnani JH, Longatto-Filho A, Reis RM, Scapulatempo-Neto C, Silveira HCS, Vidal DO, Burnette A, Eschbacher J, Hermes B, Noss A, Singh R, Anderson ML, Castro PD, Ittmann M, Huntsman D, Kohl B, Le X, Thorp R, Andry C, Duffy ER, Lyadov V, Paklina O, Setdikova G, Shabunin A, Tavobilov M, McPherson C, Warnick R, Berkowitz R, Cramer D, Feltmate C, Horowitz N, Kibel A, Muto M, Raut CP, Malykh A, Barnholtz-Sloan JS, Barrett W, Devine K, Fulop J, Ostrom QT, Shimmel K, Wolinsky Y, Sloan AE, de Rose A, Giuliante F, Goodman M, Karlan BY, Hagedorn CH, Eckman J, Harr J, Myers J, Tucker K, Zach LA, Deyarmin B, Hu H, Kvecher L, Larson C, Mural RJ, Somiari S, Vicha A, Zelinka T, Bennett J, Iacocca M, Rabeno B, Swanson P, Latour M, Lacombe L, Têtu B, Bergeron A, McGraw M, Staugaitis SM, Chabot J, Hibshoosh H, Sepulveda A, Su T, Wang T, Potapova O, Voronina O, Desjardins L, Mariani O, Roman-Roman S, Sastre X, Stern MH, Cheng F, Signoretti S, Berchuck A, Bigner D, Lipp E, Marks J, McCall S, McLendon R, Secord A, Sharp A, Behera M, Brat DJ, Chen A, Delman K, Force S, Khuri F, Magliocca K, Maithel S, Olson JJ, Owonikoko T, Pickens A, Ramalingam S, Shin DM, Sica G, van Meir EG, Zhang Hongzheng, Eijckenboom W, Gillis A, Korpershoek E, Looijenga L, Oosterhuis W, Stoop H, van Kessel KE, Zwarthoff EC, Calatozzolo C, Cuppini L, Cuzzubbo S, DiMeco F, Finocchiaro G, Mattei L, Perin A, Pollo B, Chen C, Houck J, Lohavanichbutr P, Hartmann A, Stoehr C, Stoehr R, Taubert H, Wach S, Wullich B, Kycler W, Murawa D, Wiznerowicz M, Chung K, Edenfield WJ, Martin J, Baudin E, Bubley G, Bueno R, de Rienzo A, Richards WG, Kalkanis S, Mikkelsen T, Noushmehr H, Scarpace L, Girard N, Aymerich M, Campo E, Giné E, Guillermo AL, van Bang N, Hanh PT, Phu BD, Tang Y, Colman H, Evason K, Dottino PR, Martignetti JA, Gabra H, Juhl H, Akeredolu T, Stepa S, Hoon D, Ahn K, Kang KJ, Beuschlein F, Breggia A, Birrer M, Bell D, Borad M, Bryce AH, Castle E, Chandan V, Cheville J, Copland JA, Farnell M, Flotte T, Giama N, Ho T, Kendrick

M, Kocher JP, Kopp K, Moser C, Nagorney D, O'Brien D, O'Neill BP, Patel T, Petersen G, Que F, Rivera M, Roberts L, Smallridge R, Smyrk T, Stanton M, Thompson RH, Torbenson M, Yang JD, Zhang L, Brimo F, Ajani JA, Gonzalez AMA, Behrens C, Bondaruk J, Broaddus R, Czerniak B, Esmaeli B, Fujimoto J, Gershenwald J, Guo C, Logothetis C, Meric-Bernstam F, Moran C, Ramondetta L, Rice D, Sood A, Tamboli P, Thompson T, Troncoso P, Tsao A, Wistuba I, Carter C, Haydu L, Hersey P, Jakrot V, Kakavand H, Kefford R, Lee K, Long G, Mann G, Quinn M, Saw R, Scolyer R, Shannon K, Spillane A, Stretch J, Synott M, Thompson J, Wilmott J, Al-Ahmadie H, Chan TA, Ghossein R, Gopalan A, Levine DA, Reuter V, Singer S, Singh B, Tien NV, Broudy T, Mirsaidi C, Nair P, Drwiega P, Miller J, Smith J, Zaren H, Park JW, Hung NP, Kebebew E, Linehan WM, Metwalli AR, Pacak K, Pinto PA, Schiffman M, Schmidt LS, Vocke CD, Wentzensen N, Worrell R, Yang H, Moncrieff M, Goparaju C, Melamed J, Pass H, Botnariuc N, Caraman I, Cernat M, Chemencedji I, Clipca A, Doruc S, Gorincioi G, Mura S, Pirtac M, Stancul I, Tcaciuc D, Albert M, Alexopoulou I, Arnaout A, Bartlett J, Engel J, Gilbert S, Parfitt J, Sekhon H, Thomas G, Rassl DM, Rintoul RC, Bifulco C, Tamakawa R, Urba W, Hayward N, Timmers H, Antenucci A, Facciolo F, Grazi G, Marino M, Merola R, de Krijger R, Gimenez-Roqueplo AP, Piché A, Chevalier S, McKercher G, Birsoy K, Barnett G, Brewer C, Farver C, Naska T, Pennell NA, Raymond D, Schilero C, Smolenski K, Williams F, Morrison C, Borgia JA, Liptay MJ, Pool M, Seder CW, Junker K, Omberg L, Dinkin M, Manikhas G, Alvaro D, Bragazzi MC, Cardinale V, Carpino G, Gaudio E, Chesla D, Cottingham S, Dubina M, Moiseenko F, Dhanasekaran R, Becker KF, Janssen KP, Slotta-Huspenina J, Abdel-Rahman MH, Aziz D, Bell S, Cebulla CM, Davis A, Duell R, Elder JB, Hilty J, Kumar B, Lang J, Lehman NL, Mandt R, Nguyen P, Pilarski R, Rai K, Schoenfield L, Senecal K, Wakely P, Hansen P, Lechan R, Powers J, Tischler A, Grizzle WE, Sexton KC, Kastl A, Henderson J, Porten S, Waldmann J, Fassnacht M, Asa SL, Schadendorf D, Couce M, Graefen M, Huland H, Sauter G, Schlomm T, Simon R, Tennstedt P, Olabode O, Nelson M, Bathe O, Carroll PR, Chan JM, Disaia P, Glenn P, Kelley RK, Landen CN, Phillips J, Prados M, Simko J, Smith-McCune K, VandenBerg S, Roggin K, Fehrenbach A, Kendler A, Sifri S, Steele R, Jimeno A, Carey F, Forgie I, Mannelli M, Carney M, Hernandez B, Campos B, Herold-Mende C, Jungk C, Unterberg A, von Deimling A, Bossler A, Galbraith J, Jacobus L, Knudson M, Knutson T, Ma D, Milhem M, Sigmund R, Godwin AK, Madan R, Rosenthal HG, Adebamowo C, Adebamowo SN, Boussioutas A, Beer D, Giordano T, Mes-Masson AM, Saad F, Bocklage T, Landrum L, Mannel R, Moore K, Moxley K, Postier R, Walker J, Zuna R, Feldman M, Valdivieso F, Dhir R, Luketich J, Pinero EMM, Quintero-Aguilo M, Carlotti CG, dos Santos JS, Kemp R, Sankarankuty A, Tirapelli D, Catto J, Agnew K, Swisher E, Creaney J, Robinson B, Shelley CS, Godwin EM, Kendall S, Shipman C, Bradford C, Carey T, Haddad A, Moyer J, Peterson L, Prince M, Rozek L, Wolf G, Bowman R, Fong KM, Yang I, Korst R, Rathmell WK, Fantacone-Campbell JL, Hooke JA, Kovatich AJ, Shriver CD, DiPersio J, Drake B, Govindan R, Heath S, Ley T, van Tine B, Westervelt P, Rubin MA, Lee J il, Aredes ND, Mariamidze A, van Allen EM, Cherniack AD, Ciriello G, Sander C, Schultz N. 2018. Oncogenic Signaling Pathways in The Cancer Genome Atlas. *Cell* **173**:321-337.e10. doi:10.1016/J.CELL.2018.03.035

Scheffner M, Werness BA, Huibregtse JM, Levine AJ, Howley PM. 1990. The E6 oncoprotein encoded by human papillomavirus types 16 and 18 promotes the degradation of p53. *Cell* **63**:1129–1136. doi:10.1016/0092-8674(90)90409-8

1158 Schlegelmilch K, Mohseni M, Kirak O, Pruszak J, Rodriguez JR, Zhou D, Kreger BT, Vasioukhin
1159 V, Avruch J, Brummelkamp TR, Camargo FD. 2011. Yap1 acts downstream of α-catenin to
1160 control epidermal proliferation. *Cell* **144**:782–795. doi:10.1016/j.cell.2011.02.031

1161 Seavey SE, Holubar M, Saucedo LJ, Perry ME. 1999. The E7 Oncoprotein of Human
1162 Papillomavirus Type 16 Stabilizes p53 through a Mechanism Independent of p19ARF.
1163 *Journal of Virology* **73**:7590–7598. doi:10.1128/jvi.73.9.7590-7598.1999

1164 Shanzer M, Ricardo-Lax I, Keshet R, Reuven N, Shaul Y. 2015. The polyomavirus middle T-
1165 antigen oncogene activates the Hippo pathway tumor suppressor Lats in a Src-dependent
1166 manner. *Oncogene* **34**:4190–4198. doi:10.1038/onc.2014.347

1167 Strati K, Lambert PF. 2007. Role of Rb-dependent and Rb-independent functions of
1168 papillomavirus E7 oncogene in head and neck cancer. *Cancer Research* **67**:11585–11593.
1169 doi:10.1158/0008-5472.CAN-07-3007

1170 Styles CT, Bazot Q, Parker GA, White RE, Paschos K, Allday MJ. 2017. EBV epigenetically
1171 suppresses the B cell-to-plasma cell differentiation pathway while establishing long-term
1172 latency. *PLOS Biology* **15**:e2001992. doi:10.1371/JOURNAL.PBIO.2001992

1173 Szalmás A, Tomaić V, Basukala O, Massimi P, Mittal S, Kónya J, Banks L. 2017. The PTPN14
1174 Tumor Suppressor Is a Degradation Target of Human Papillomavirus E7. *Journal of*
1175 *Virology* **91**:e00057-17. doi:10.1128/jvi.00057-17

1176 Szymaniak AD, Mahoney JE, Cardoso W v., Varelas X. 2015. Crumbs3-Mediated Polarity
1177 Directs Airway Epithelial Cell Fate through the Hippo Pathway Effector Yap. *Developmental*
1178 *Cell* **34**:283–296. doi:10.1016/J.DEVCEL.2015.06.020

1179 Tian Y, Li D, Dahl J, You J, Benjamin T. 2004. Identification of TAZ as a Binding Partner of the
1180 Polyomavirus T Antigens. *Journal of Virology* **78**:12657–12664.
1181 doi:10.1128/jvi.78.22.12657-12664.2004

1182 Totaro A, Castellan M, Battilana G, Zanconato F, Azzolin L, Giulitti S, Cordenonsi M, Piccolo S.
1183 2017. YAP/TAZ link cell mechanics to Notch signalling to control epidermal stem cell fate.
1184 *Nature Communications* **8**:1–13. doi:10.1038/ncomms15206

1185 Wang H-K, Duffy AA, Broker TR, Chow LT. 2009. Robust production and passaging of
1186 infectious HPV in squamous epithelium of primary human keratinocytes. *Genes &*
1187 *development* **23**:181–94. doi:10.1101/gad.1735109

1188 Wang S, Drummond ML, Guerrero-Juarez CF, Tarapore E, MacLean AL, Stabell AR, Wu SC,
1189 Gutierrez G, That BT, Benavente CA, Nie Q, Atwood SX. 2020. Single cell transcriptomics
1190 of human epidermis identifies basal stem cell transition states. *Nature Communications*
1191 *2020 11:1* **11**:1–14. doi:10.1038/s41467-020-18075-7

1192 Wang W, Huang J, Wang X, Yuan J, Li X, Feng L, Park J il, Chen J. 2012. PTPN14 is required
1193 for the density-dependent control of YAP1. *Genes and Development* **26**:1959–1971.
1194 doi:10.1101/gad.192955.112

1195 Wang Z, Lu W, Zhang Y, Zou F, Jin Z, Zhao T. 2020. The Hippo Pathway and Viral Infections.
1196 *Frontiers in Microbiology* **0**:3033. doi:10.3389/FMICB.2019.03033

Webb Strickland S, Brimer N, Lyons C, vande Pol SB. 2018. Human Papillomavirus E6 interaction with cellular PDZ domain proteins modulates YAP nuclear localization. *Virology* **516**:127–138. doi:10.1016/J.VIROL.2018.01.003

Werness BA, Levine AJ, Howley PM. 1990. Association of human papillomavirus types 16 and 18 E6 proteins with p53. *Science* **248**:76–79. doi:10.1126/science.2157286

White EA, Kramer RE, Hwang JH, Pores Fernando AT, Naetar N, Hahn WC, Roberts TM, Schaffhausen BS, Livingston DM, Howley PM. 2015. Papillomavirus E7 Oncoproteins Share Functions with Polyomavirus Small T Antigens. *Journal of Virology* **89**:2857–2865. doi:10.1128/jvi.03282-14

White EA, Kramer RE, Tan MJA, Hayes SD, Harper JW, Howley PM. 2012a. Comprehensive Analysis of Host Cellular Interactions with Human Papillomavirus E6 Proteins Identifies New E6 Binding Partners and Reflects Viral Diversity. *Journal of Virology* **86**:13174–13186. doi:10.1128/JVI.02172-12

White EA, Münger K, Howley PM. 2016. High-Risk Human Papillomavirus E7 Proteins Target PTPN14 for Degradation. *mBio* **7**:e01530-16. doi:10.1128/mBio.01530-16

White EA, Sowa ME, Tan MJA, Jeudy S, Hayes SD, Santha S, Münger K, Harper JW, Howley PM. 2012b. Systematic identification of interactions between host cell proteins and E7 oncoproteins from diverse human papillomaviruses. *Proceedings of the National Academy of Sciences of the United States of America* **109**:E260-7. doi:10.1073/pnas.1116776109

Yimlamai D, Christodoulou C, Galli GG, Yanger K, Pepe-Mooney B, Gurung B, Shrestha K, Cahan P, Stanger BZ, Camargo FD. 2014. Hippo Pathway Activity Influences Liver Cell Fate. *Cell* **157**:1324–1338. doi:10.1016/J.CELL.2014.03.060

You J, Croyle JL, Nishimura A, Ozato K, Howley PM. 2004. Interaction of the bovine papillomavirus E2 protein with Brd4 tethers the viral DNA to host mitotic chromosomes. *Cell* **117**:349–360. doi:10.1016/S0092-8674(04)00402-7

Yuan Y, Park J, Feng A, Awasthi P, Wang Z, Chen Q, Iglesias-Bartolome R. 2020. YAP1/TAZ-TEAD transcriptional networks maintain skin homeostasis by regulating cell proliferation and limiting KLF4 activity. *Nature Communications* **11**:1–14. doi:10.1038/s41467-020-15301-0

Yuan Y, Salinas Parra N, Chen Q, Iglesias-Bartolome R. 2021. Oncogenic Hedgehog-Smoothened Signaling Depends on YAP1–TAZ/TEAD Transcription to Restrain Differentiation in Basal Cell Carcinoma. *Journal of Investigative Dermatology*. doi:10.1016/J.JID.2021.06.020

Yun H-Y, Kim MW, Lee HS, Kim W, Shin JH, Kim H, Shin H-C, Park H, Oh B-H, Kim WK, Bae K-H, Lee SC, Lee E-W, Ku B, Kim SJ. 2019. Structural basis for recognition of the tumor suppressor protein PTPN14 by the oncoprotein E7 of human papillomavirus. *PLOS Biology* **17**:e3000367. doi:10.1371/journal.pbio.3000367

Zhang H, Pasolli HA, Fuchs E. 2011. Yes-associated protein (YAP) transcriptional coactivator functions in balancing growth and differentiation in skin. *Proceedings of the National Academy of Sciences* **108**:2270–2275. doi:10.1073/pnas.1019603108

Zhao B, Wei X, Li W, Udan RS, Yang Q, Kim J, Xie J, Ikenoue T, Yu J, Li L, Zheng P, Ye K, Chinnaiyan A, Halder G, Lai Z-C, Guan K-L. 2007. Inactivation of YAP oncoprotein by the Hippo pathway is involved in cell contact inhibition and tissue growth control. *Genes & Development* **21**:2747–2761. doi:10.1101/GAD.1602907

Zhao R, Fallon TR, Saladi SV, Pardo-Saganta A, Villoria J, Mou H, Vinarsky V, Gonzalez-Celeiro M, Nunna N, Hariri LP, Camargo F, Ellisen LW, Rajagopal J. 2014. Yap Tunes Airway Epithelial Size and Architecture by Regulating the Identity, Maintenance, and Self-Renewal of Stem Cells. *Developmental Cell* **30**:151–165. doi:10.1016/j.devcel.2014.06.004

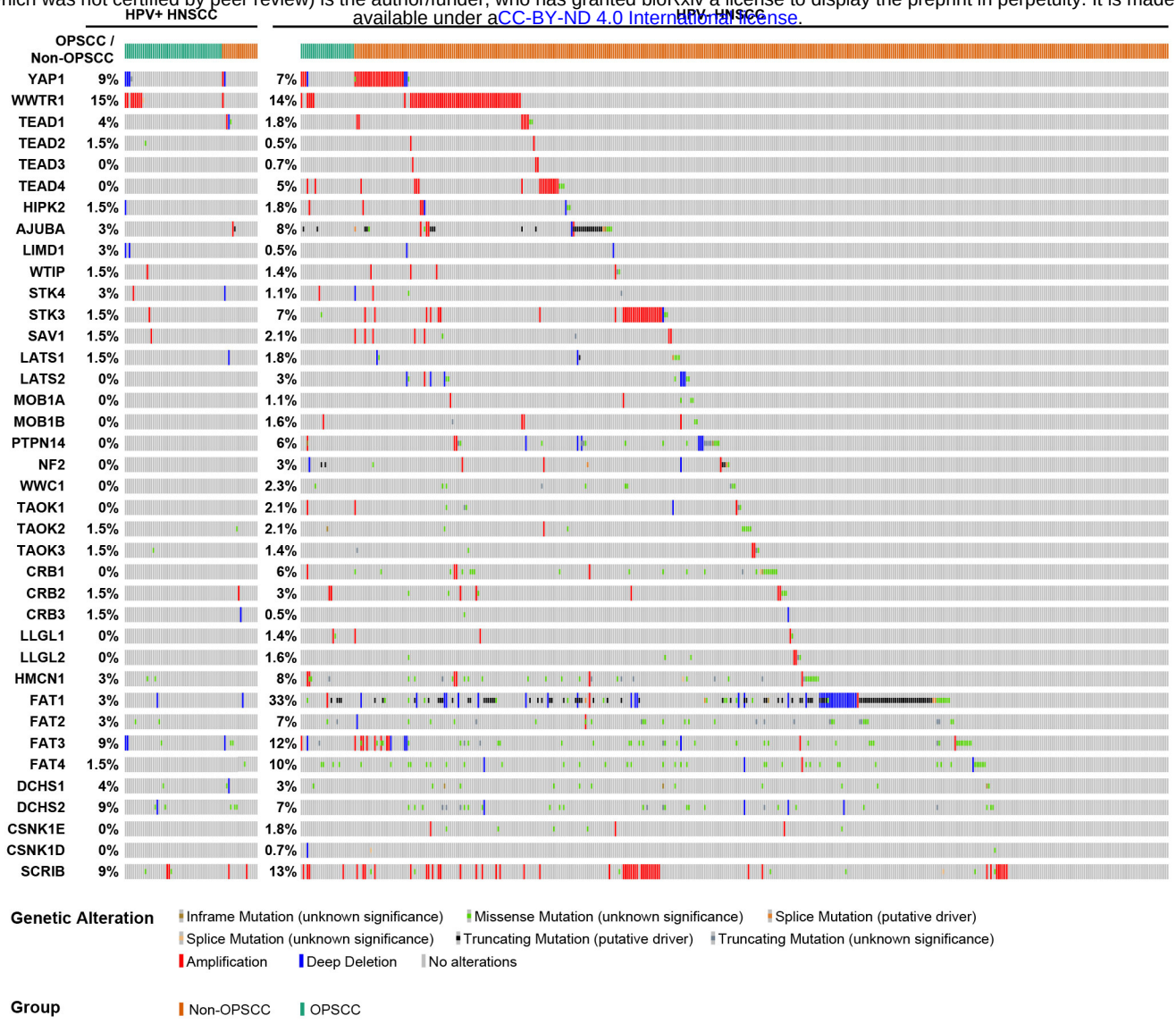

Figure 1—figure supplement 1 | HPV-positive HNSCC have fewer Hippo pathway alterations and lower expression of differentiation genes. cBioPortal analysis for genomic mutations and copy number alterations in HPV+/- HNSCC and OPSCC. Oncoprint displays specific genomic alterations in individual tumor samples.

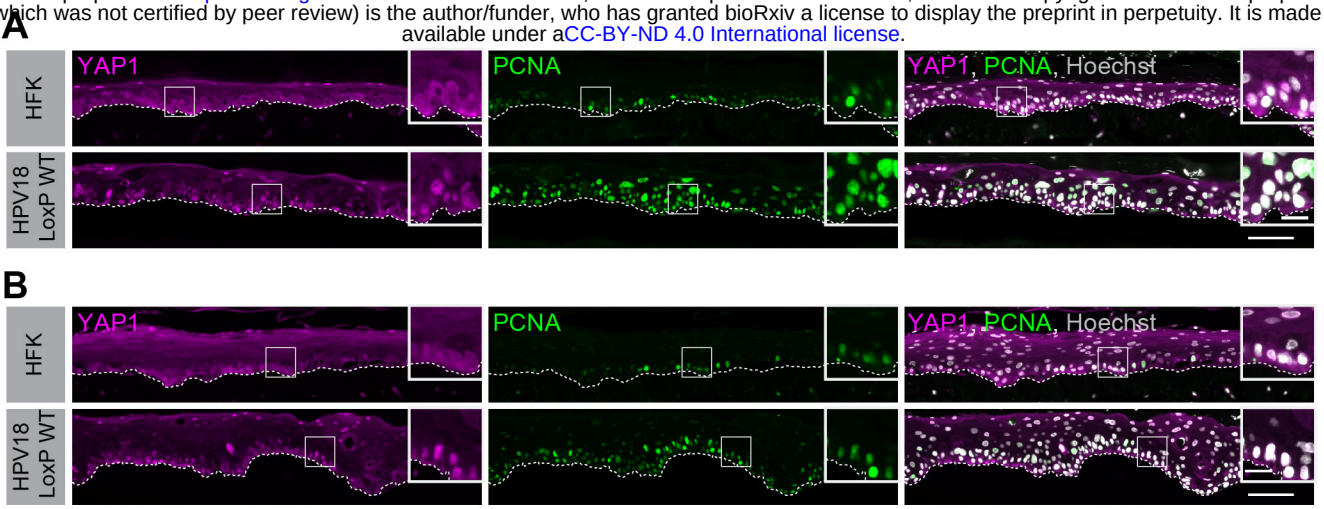

Figure 1—figure supplement 2 | HPV18 E7 activates YAP1 in basal keratinocytes. (A-B) Additional replicates of organotypic cultures grown from primary HFK or HFK harboring the HPV18 genome. FFPE sections were stained for YAP1 (magenta), PCNA (green), and Hoechst (gray). White dashed lines indicate the basement membrane. White boxes indicate the location of insets in main images. Main image scale bars = 100 μm. Inset scale bars = 25 μm.

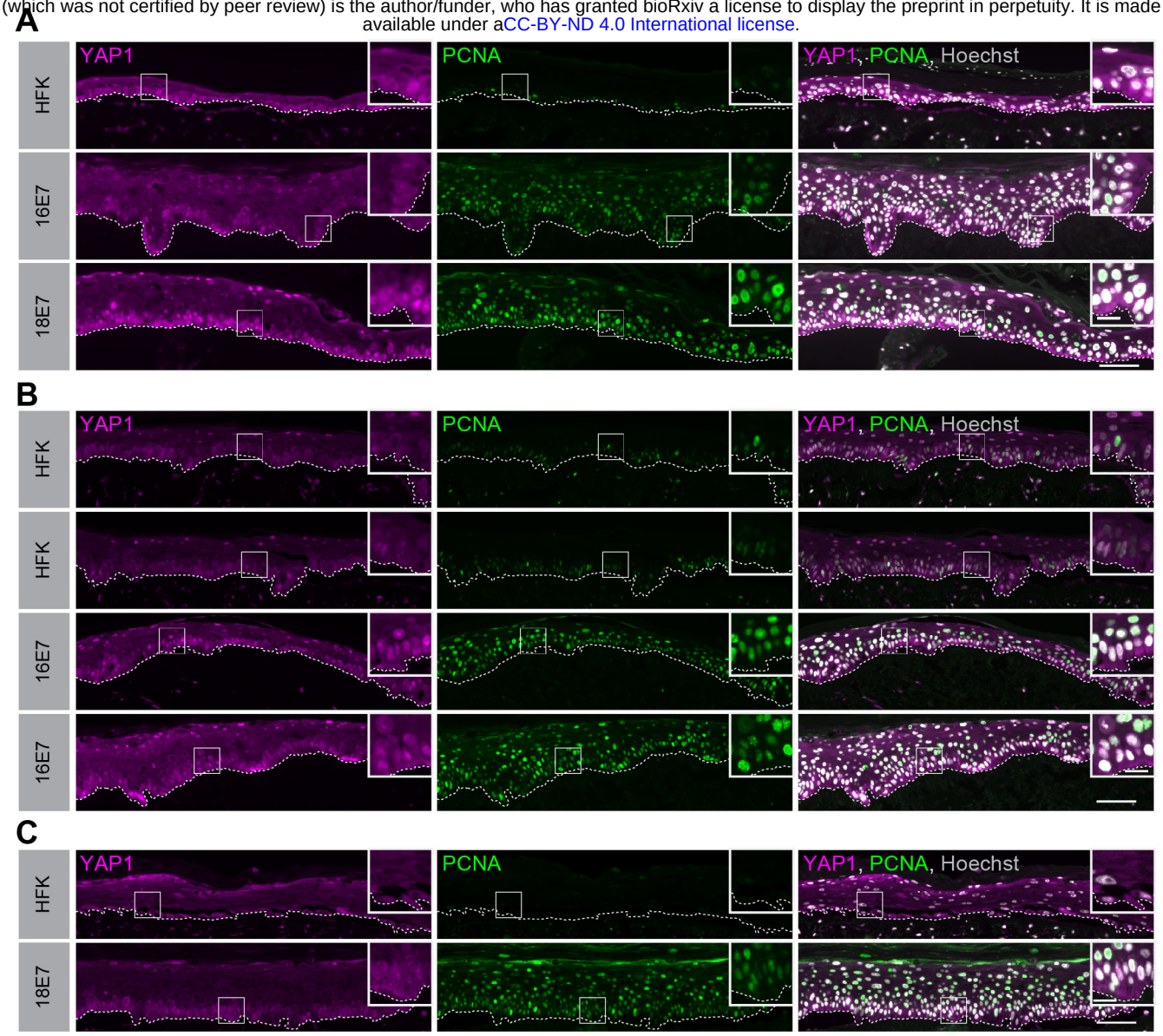

Figure 1—figure supplement 3 | HPV E7 activates YAP1 in basal keratinocytes. Additional replicates of organotypic cultures grown from primary HFK or HFK transduced with retroviral expression encoding HPV E7 proteins. FFPE sections of cultures grown from (A) HFK or HFK expressing HPV16 E7 or HPV18 E7, (B) HFK or HFK transduced with HPV16 E7, or (E) HFK and HFK expressing HPV18 E7 were stained for YAP1 (magenta), PCNA (green), and Hoechst (gray). White dashed lines indicate the basement membrane. White boxes indicate the location of insets in main images. Main image scale bars = 100 μm. Inset scale bars = 25 μm.

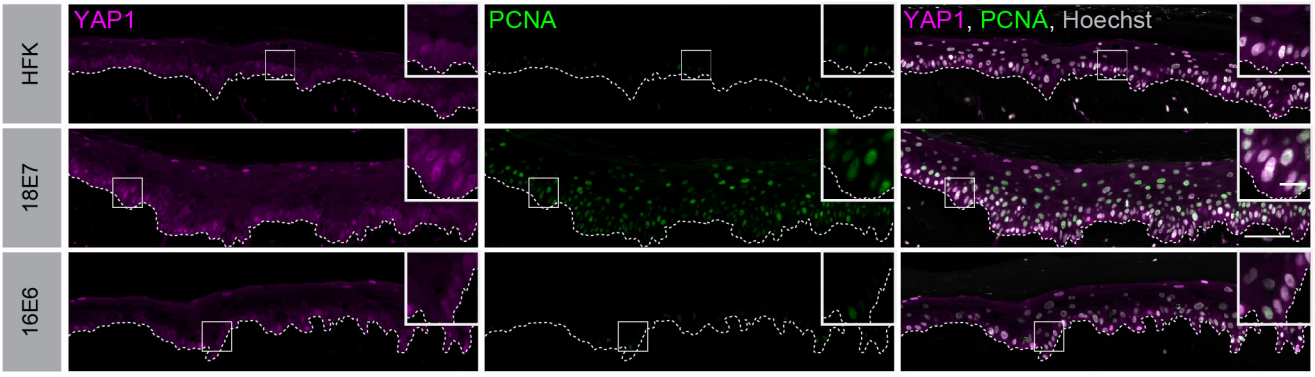

Figure 1—figure supplement 4 | HPV E6 does not activate YAP1 in basal keratinocytes. Additional replicates of organotypic cultures grown from primary HFK or HFK transduced with retroviral expression encoding HPV E6 or E7 proteins. FFPE sections were stained for YAP1 (magenta), PCNA (green), and Hoechst (gray). White dashed lines indicate the basement membrane. White boxes indicate the location of insets in main images. Main image scale bars = 100 μm. Inset scale bars = 25 μm.

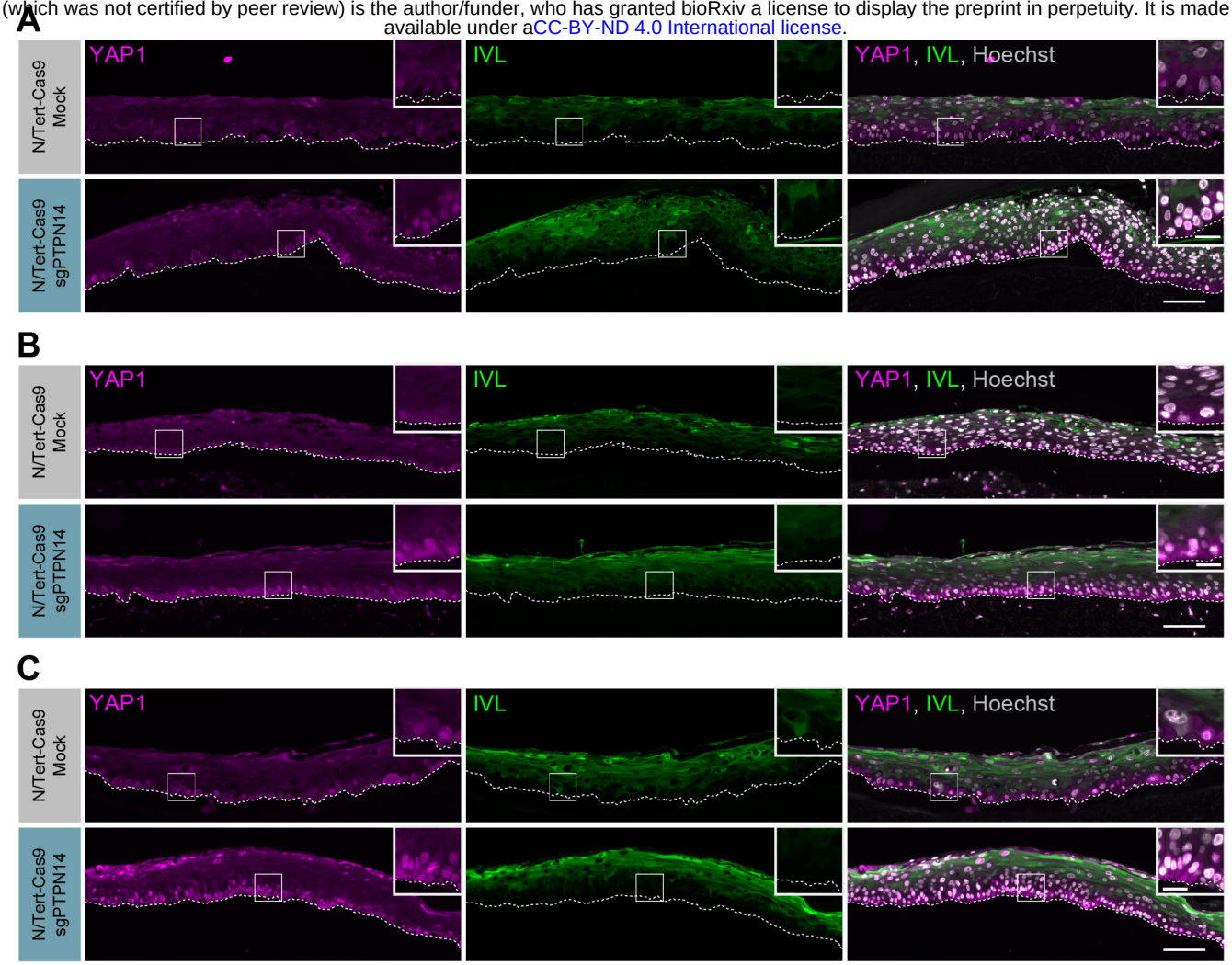

Figure 2—figure supplement 1 | PTPN14 knockout activates YAP1 in basal keratinocytes. Additional replicates of organotypic cultures grown from N/Tert-Cas9 keratinocytes (A-C) FFPE sections from mock or sgPTPN14 transfected N/Tert-Cas9 keratinocytes were stained for YAP1 (magenta), IVL (green), and Hoechst (Gray). White dashed lines indicate the basement membrane. White boxes indicate the location of insets in main images. Main image scale bars = 100 μm. Inset scale bars = 25 μm.

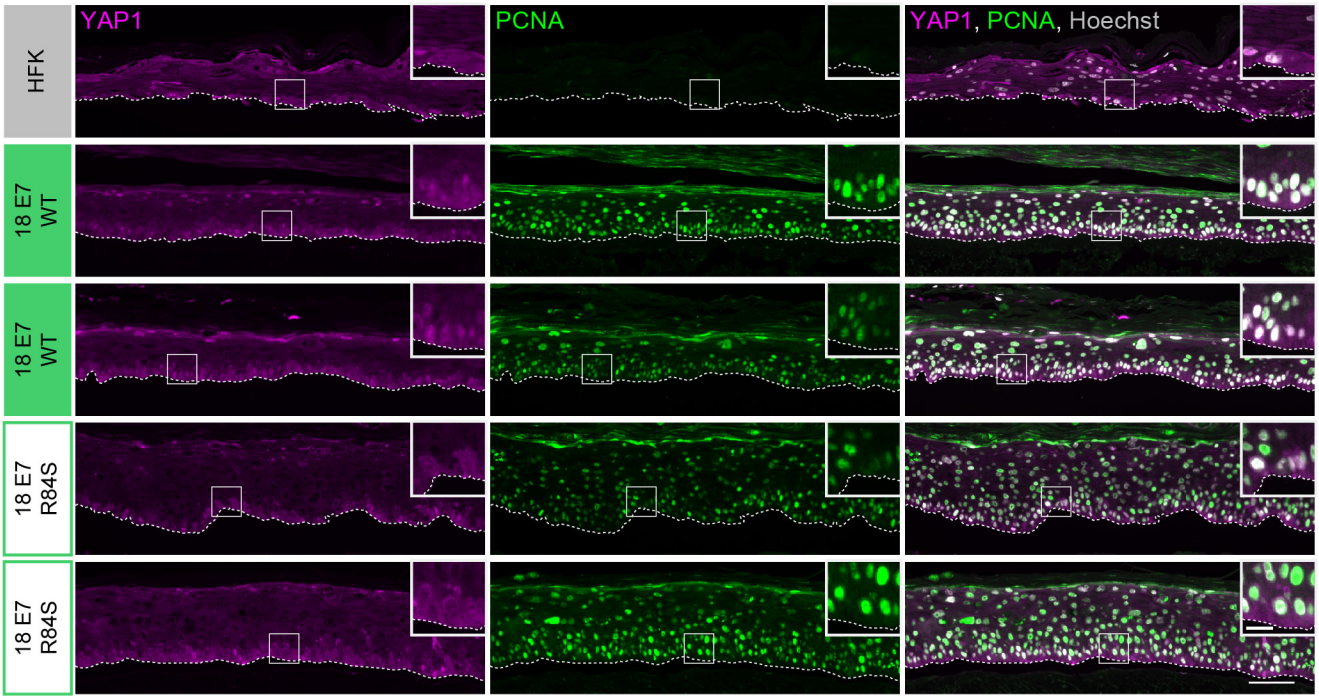

Figure 2—figure supplement 2 | HPV E7 activates YAP1 in basal keratinocytes through PTPN14 degradation. Additional replicates of organotypic cultures grown from primary HFK transduced with retroviral expression vectors encoding HPV18 E7 WT or R84S. FFPE sections from parental HFK, HPV18 E7 WT or HPV18 E7 R84S expressing HFK were stained for YAP1 (magenta), PCNA (green), and Hoechst (Gray). White dashed lines indicate the basement membrane. White boxes indicate the location of insets in main images. Main image scale bars = 100 μm. Inset scale bars = 25 μm.

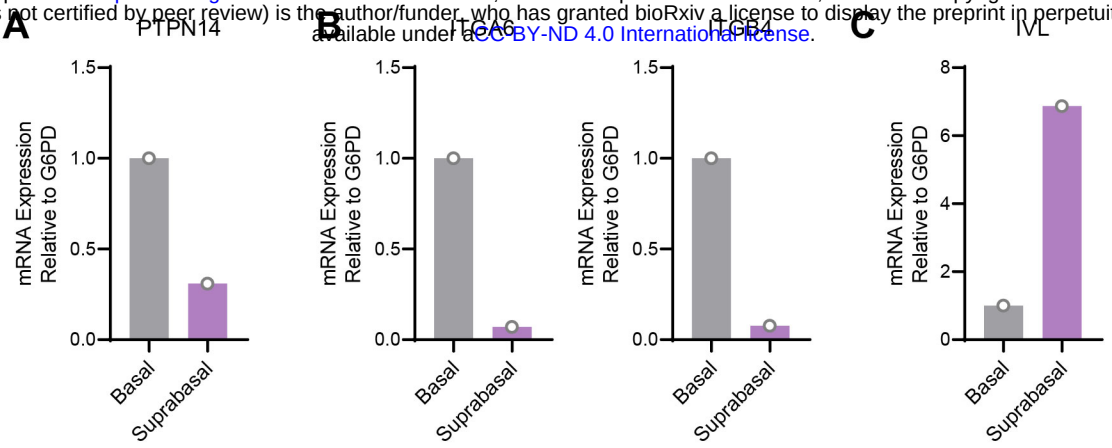

Figure 3—figure supplement 1 | PTPN14 expression is enriched in basal keratinocytes in HPV 18 E7 expressing organotypic cultures. Basal and suprabasal layers from a 3D organotypic culture grown from HFK transduced with a retroviral expression vector encoding HPV18 E7 were dissected using laser capture microdissection. RNA was purified from isolated layers and qRT-PCR was used to assess the expression of PTPN14 (A), the basal cell markers ITGA6 and ITGB4 (B), and the differentiation marker IVL (C). Graphs display individual data points.

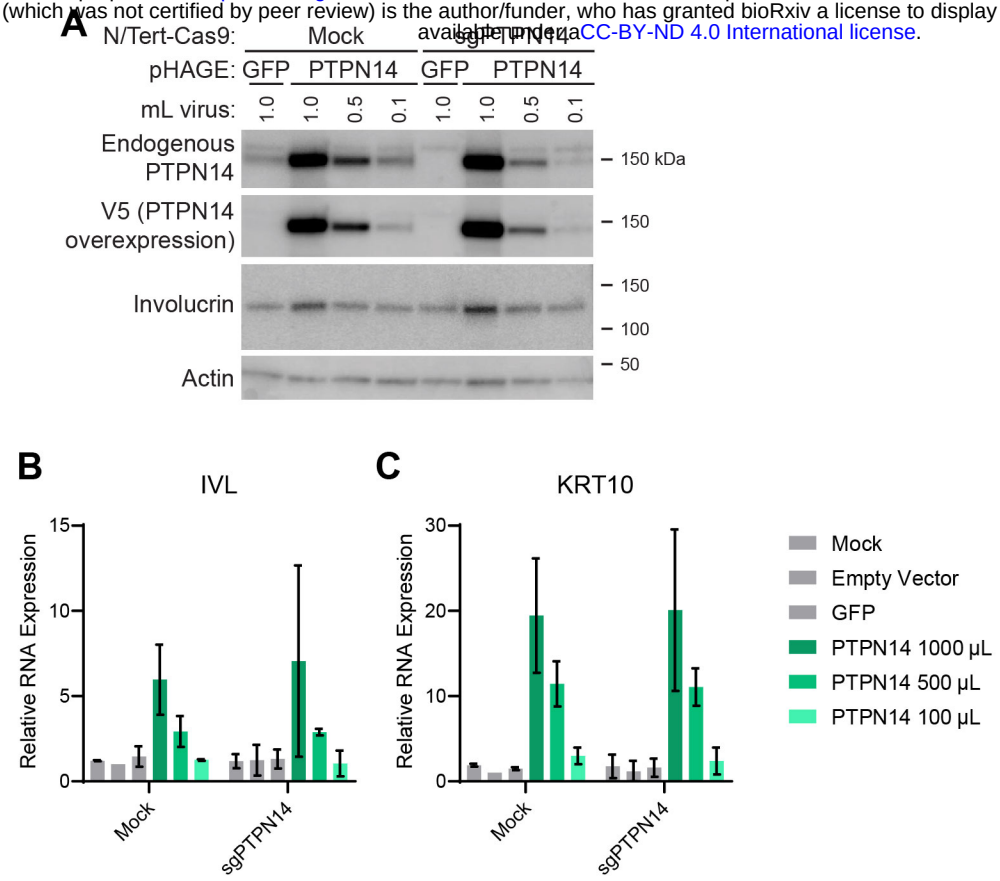

Figure 4—figure supplement 1 | PTPN14 overexpression promotes differentiation in keratinocytes. NTert-Cas9 Mock and sgPTPN14-1 keratinocytes were transduced with lentiviruses encoding GFP or PTPN14 or the empty vector control. (A) Cell lysates were subjected to SDS/PAGE/Western analysis and probed with antibodies to PTPN14, V5-tag, Involucrin, and Actin. (B) qRT-PCR was used to measure the expression of the differentiation markers IVL and KRT10 relative to G6PD. Graphs display the mean ± SD of two independent replicates.

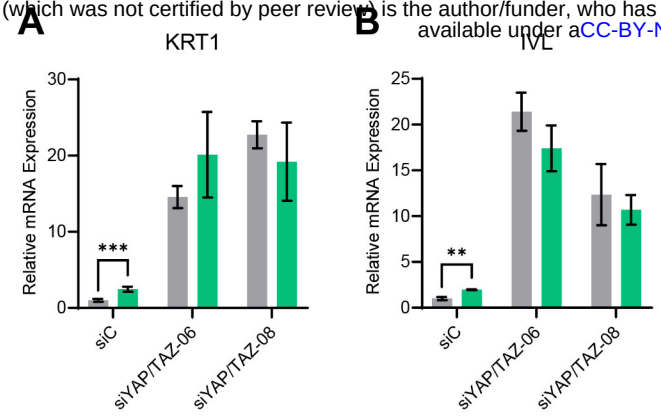

Figure 4—figure supplement 2 | YAP1 and TAZ are required for PTPN14 to promote keratinocyte differentiation. Primary HFK were transfected with control or YAP1 and WWTR1 targeting siRNAs then transduced with PTPN14 encoding lentivirus. qRT-PCR was used to measure the expression of the differentiation markers (A) KRT1 and (B) IVL relative to G6PD. Graphs portray the change in gene expression relative to siC. Graphs display the mean ± SD of three independent replicates. Statistical significance was determined by ANOVA (**p<0.01, ***p<0.001).

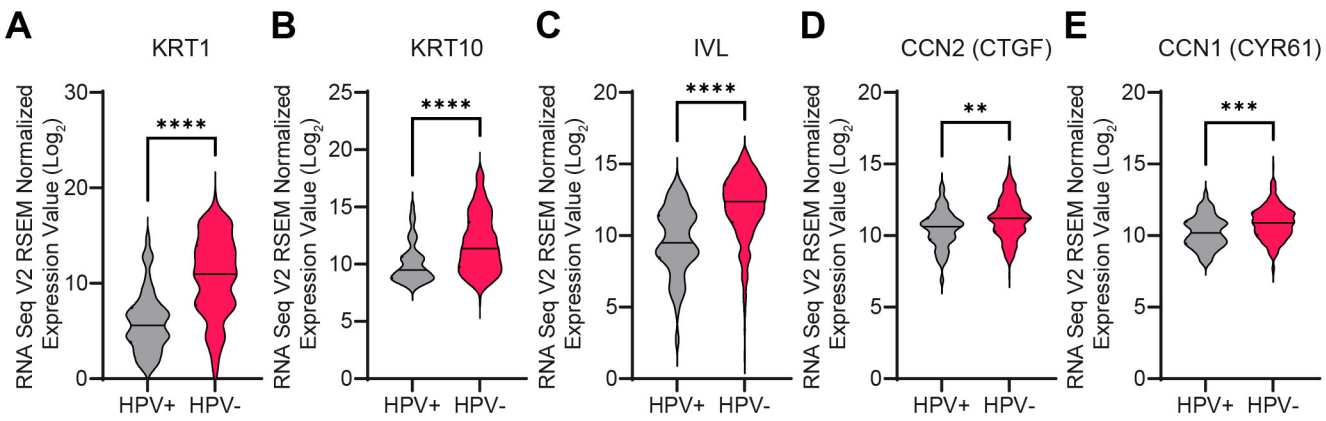

Figure 5—figure supplement 1 | HPV-positive HNSCC express lower levels of differentiation genes. RNA-seq data from TCGA were accessed through cBioPortal. Violin plots display the distribution in log2 mRNA expression of differentiation markers (A) KRT1, (B) KRT10, and (C) IVL, and the canonical YAP1/TAZ targets (D) CTGF and (E) CYR61. Statistical significance was determined by Mann-Whitney nonparametric test. (**p<0.01, ***p<0.001, ****p<0.0001).

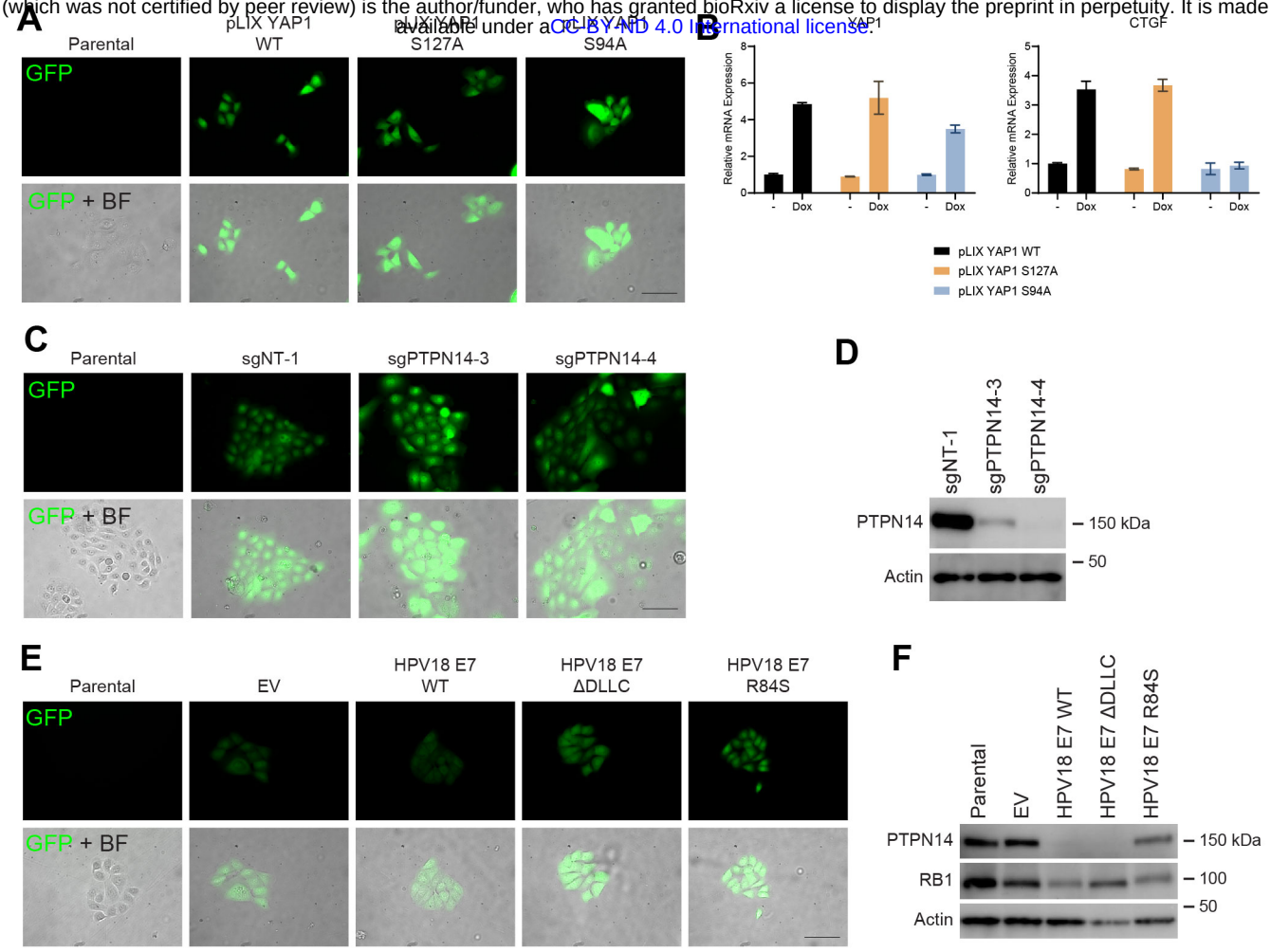

Figure 7—figure supplement 1 | PTPN14 degradation by HPV E7 promotes basal cell retention. (A-B) GFP-labeled HFK were transduced with YAP1 WT, YAP1 S127A, or YAP1 S94A under the control of a doxycycline inducible promoter. (A) GFP expression was confirmed by fluorescence microscopy. Scale bar = 100 μm. (B) Total RNA was purified from monolayer cells +/- treatment with 1 μg/mL doxycycline for 72h. qRT-PCR was used to assess gene expression of YAP1 and CTGF. (C-D) GFP-labeled HFK were transduced with retroviral vectors encoding HPV18 WT, HPV18 ΔDLLC, HPV18 E7 R84S, or the empty vector control (EV). (C) GFP expression was confirmed by fluorescence microscopy. Scale bar = 100 μm. (D) Cell lysates were subjected to SDS/PAGE/Western analysis and probed with antibodies to PTPN14, RB1, and Actin. (E-F) GFP-labeled HFK were transduced with LentiCRISPR v2 sgNT-1, sgPTPN14-3, or sgPTPN14-4 vectors. (E) GFP expression was confirmed by fluorescence microscopy. Scale bar = 100 μm (F) Cell lysates were subjected to SDS/PAGE/Western analysis and probed with antibodies to PTPN14 and Actin.

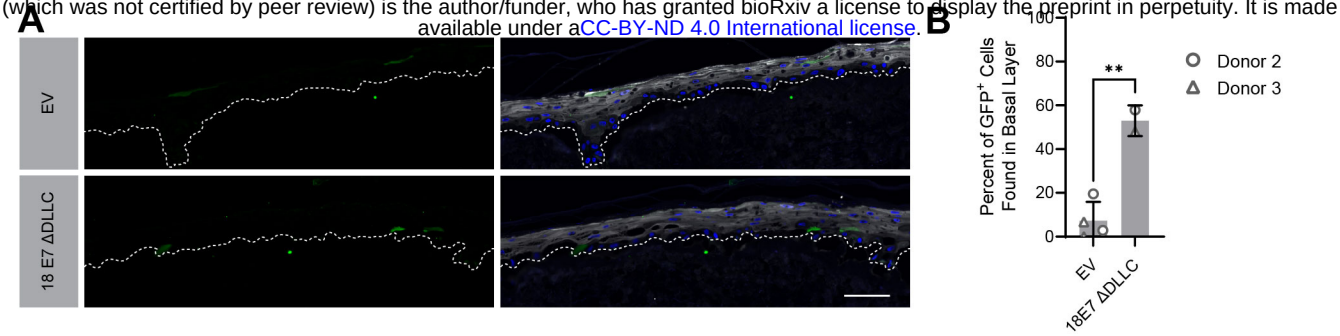

Figure 7—figure supplement 2 | HPV18 E7 can promote basal cell retention in the absence of RB1 binding. Organotypic cultures were grown from GFP-labeled cells mixed with unmodified HFK. GFP-labeled HFK were transduced with HPV18 E7 ΔDLLC or the empty vector (EV). GFP-labeled cells were mixed 1:50 into unmodified HFK. (A) FFPE sections were stained for GFP (green), IVL (grey), and Hoechst (blue). Scale bar = 100 μm (B) Quantification of the percentage of GFP+ cells found in the basal layer. Graphs display the mean ± SD and each individual data point (independent cultures). Statistical significance was determined by t-test. (**p<0.01).

Key Resources Table

Reagent type (species) or resource	Designation	Source or reference	Identifiers	Additional information
antibody	anti-Actin (Mouse monoclonal)	Sigma-Aldrich	Cat#: MAB1501	WB (1:20,000)
antibody	anti-GFP (Rabbit polyclonal)	Invitrogen	Cat#: A6455	WB (1:1,000); IHC-P (1:2000)
antibody	anti-Mouse IgG Alexa Fluor 488 (Goat polyclonal)	Invitrogen	Cat#: A11001	IHC-P (1:250)
antibody	anti-Mouse IgG HRP (Horse monoclonal)	Cell Signaling Technologies	Cat#: 7076	WB (1:2000)
antibody	anti-Rabbit IgG Alexa Fluor 594 (Goat polyclonal)	Invitrogen	Cat#: A11012	IHC-P (1:250)
antibody	anti-Rabbit IgG HRP (Goat monoclonal)	Cell Signaling Technologies	Cat#: 7074	WB (1:2000)
antibody	anti-HA-Peroxidase (Rat monoclonal)	Roche	Cat#: 12013819001	WB (1:500)
antibody	anti-ITGB4 (Rabbit polyclonal)	Sigma-Aldrich	Cat#: HPA036348	IHC-P (1:100)
antibody	anti-IVL (Mouse monoclonal)	Santa Cruz Biotechnology	Cat#: sc-398952	IHC-P (1:100)
antibody	anti-KRT1 (Mouse monoclonal	Enzo Life Sciences	Cat#: C34904	
antibody	anti-PCNA	Santa Cruz Biotechnology	Cat#: sc-56	IHC-P (1:100)

antibody	Anti-PTPN14 (Rabbit monoclonal)	Cell Signaling Technology	D5T6Y; Cat#: 13808	WB (1:500)
antibody	anti-TAZ (Rabbit monoclonal)	Cell Signaling Technology	D3I6D; Cat#: 70148	WB (1:1000)
antibody	anti-V5 (Mouse monoclonal)	Invitrogen	Cat#: 46-0705	WB (1:1000)
antibody	anti-YAP1 (Rabbit monoclonal)	Cell Signaling Technology	D8H1X; Cat#: 14074	WB (1:1000); IHC-P (1:50)
transfected construct (human)	nontargeting siRNA	Dharmacon	Cat#: D-001810-01	
transfected construct (human)	siRNA to YAP1 (OnTarget Plus)	Dharmacon	Cat#: J-012200-06	
transfected construct (human)	siRNA to YAP1 (OnTarget Plus)	Dharmacon	Cat#: J-012200-08	
transfected construct (human)	siRNA to WWTR1 (OnTarget Plus)	Dharmacon	Cat#: J-016083-06	
transfected construct (human)	siRNA to WWTR1 (OnTarget Plus)	Dharmacon	Cat#: J-016083-08	
transfected construct (human)	siRNA to PTPN14 (OnTarget Plus)	Dharmacon	Cat#: J-008509-05	
transfected construct (human)	siRNA to PTPN14 (OnTarget Plus)	Dharmacon	Cat#: J-008509-08	
transfected construct (human)	siRNA to LATS1 (OnTarget Plus)	Dharmacon	Cat#: J-004632-05	
transfected construct (human)	siRNA to LATS1 (OnTarget Plus)	Dharmacon	Cat#: J-004632-08	

transfected construct (human)	siRNA to LATS2 (OnTarget Plus)	Dharmacon	Cat#: J-003865-09	
transfected construct (human)	siRNA to LATS2 (OnTarget Plus)	Dharmacon	Cat#: J-003865-10	

Supplemental File 1
Plasmids used in the study

White lab

plasmid #	Plasmid name	Gene	Promoter	Bacterial Resistance	Tag	Tag location	Selectable Marker	Addgene Number	Original Source
8130	MSCV GFP Puro C-FlagHA	GFP	MSCV LTR	Ampicillin	Flag, HA	C terminus	Puromycin	n/a	This Study
6640	MSCV-P C-FlagHA 16E7	HPV16 E7	MSCV LTR	Ampicillin	Flag, HA	C terminus	Puromycin	35018	White et al. (2012) PNAS: 109(5):E260–E267
6641	MSCV-P C-FlagHA 18E7	HPV18 E7	MSCV LTR	Ampicillin	Flag, HA	C terminus	Puromycin	35019	White et al. (2012) PNAS: 109(5):E260–E267
8193	MSCV-P C-FlagHA 18E7 R84S	HPV18 E7	MSCV LTR	Ampicillin	Flag, HA	C terminus	Puromycin	163307	Hatterschide et al. (2020) J. Virol. 94:e1024-20
6659	MSCV-IP N-FlagHA 16E6	HPV16 E6	MSCV LTR	Ampicillin	Flag, HA	N terminus	Puromycin	44152	White et al. (2012) J Virol. 86(24):13174-86
8208	MSCV-Neo C-HA Empty	Empty	MSCV LTR	Ampicillin	HA	C terminus	Neomycin	163310	Hatterschide et al. (2020) J. Virol. 94:e1024-20
8133	MSCV GFP Neo C-HA	GFP	MSCV LTR	Ampicillin	HA	C terminus	Neomycin	n/a	This Study
6993	MSCV-Neo C-HA 18E7	HPV18 E7	MSCV LTR	Ampicillin	HA	C terminus	Neomycin	163311	Hatterschide et al. (2020) J. Virol. 94:e1024-20
8220	MSCV-Neo C-HA 18E7 R84S	HPV18 E7	MSCV LTR	Ampicillin	HA	C terminus	Neomycin	163312	Hatterschide et al. (2020) J. Virol. 94:e1024-20
8291	MSCV-Neo C-HA 18E7 ΔDLLC	HPV18 E7	MSCV LTR	Ampicillin	HA	C terminus	Neomycin	n/a	This Study
8340	pLenti CMV GFP Hygro (656-4)	GFP	CMV	Ampicillin	n/a	n/a	Hygromycin	17446	Campeau et al. (2009) PLoS One. 4(8):e6529
6571	PHAGE-P-CMVt N-HA GFP	GFP	CMV	Ampicillin	HA	N terminus	Puromycin	n/a	Galligan et al. (2015) J Proteome Res. 14(2): 953–966.
7522	pHAGE-P N-V5 PTPN14	PTPN14	CMV	Ampicillin	V5	N terminus	Puromycin	n/a	White et al. (2016) mBio. 7(5):e01530-16
8251	pQCXIH-Myc-YAP	YAP1 isoform 3	CMV	Ampicillin	Myc	C terminus	Hygromycin	33091	Zhao et al. (2007) Genes Dev. 21(21):2747-61
8252	pQCXIH-FLAG-YAP S127A	YAP1 isoform 3	CMV	Ampicillin	Flag	C terminus	Hygromycin	33092	Zhao et al. (2007) Genes Dev. 21(21):2747-61
8254	pQCXIH-Myc-YAP S94A	YAP1 isoform 3	CMV	Ampicillin	Myc	C terminus	Hygromycin	33094	Zhao et al. (2007) Genes Dev. 21(21):2747-61
8319	pDONR ATG-YAP1 WT-Stop	YAP1 isoform 3	n/a	Spectinomycin	n/a	n/a	n/a	n/a	This Study
8321	pDONR ATG-YAP1 S127A-Stop	YAP1 isoform 3	n/a	Spectinomycin	n/a	n/a	n/a	n/a	This Study
8322	pDONR ATG-YAP1 S94A-Stop	YAP1 isoform 3	n/a	Spectinomycin	n/a	n/a	n/a	n/a	This Study
8325	pLIX YAP1 WT	YAP1 isoform 3	TRE promoter, Tet ON	Ampicillin	n/a	n/a	Puromycin	n/a	This Study
8327	pLIX YAP1 S127A	YAP1 isoform 3	TRE promoter, Tet ON	Ampicillin	n/a	n/a	Puromycin	n/a	This Study
8328	pLIX YAP1 S94A	YAP1 isoform 3	TRE promoter, Tet ON	Ampicillin	n/a	n/a	Puromycin	n/a	This Study
8278	pInducer20 EGFP-TEADi	EGFP-TEADi	TRE promoter, Tet ON	Ampicillin	GFP	C terminus	Neomycin	140145	Yuan et al. (2020) Nat Commun. 11, 1472

White lab

plasmid #	Plasmid name	HPV genome	Bacterial Resistance	Selectable Marker	Original source
8216	pNeo-loxP-HPV18	HPV18	Kanamycin	Neomycin	Wang et al. (2009) Genes Dev. 23:181-94.

White lab

plasmid #	Plasmid name	sgRNA sequence from Broad Brunello library	Promoter	Bacterial Resistance	Selectable Marker	Addgene Number	Original Source
8092	LentiCRISPR v2 sgNT-1	AGCTCGCCATGTCGGTTCTC	U6	Ampicillin	Puromycin	163315	Hatterschide et al. (2020) J. Virol. 94:e1024-20
8115	LentiCRISPR v2 sgPTPN14-3	CCACACTGGACGTGAACGGG	U6	Ampicillin	Puromycin	163314	Hatterschide et al. (2019) PNAS: 116:7033–7042
8116	LentiCRISPR v2 sgPTPN14-4	TGTGCTTACCGTGTGAAAGA	U6	Ampicillin	Puromycin	163316	Hatterschide et al. (2020) J. Virol. 94:e1024-20

Supplemental File 1
Antibodies used in the study

Target	Antiboty Name	Company	Product Number	Use	Dilution	Notes
Actin	Anti-Actin Antibody, clone C4	Sigma-Aldrich	MAB1501	Western Blot	1:20000	
GFP	GFP Polyclonal Antibody	Invitrogen	A6455	IHC-P	1:2000	HIER: 10 mM Sodium Citrate pH 6
GFP	GFP Polyclonal Antibody	Invitrogen	A6455	Western Blot	1:1000	
Goat anti-Mouse IgG 488	Goat anti-Mouse IgG (H+L) Alexa Fluor 488	Invitrogen	A11001	IHC-P	1:250	
Goat anti-mouse IgG HRP	Anti-mouse IgG, HRP-linked Antibody	Cell Signaling Technology	7076	Western Blot	1:2000	
Goat anti-Rabbit IgG 594	Goat anti-Rabbit IgG (H+L) Alexa Fluor 594	Invitrogen	A11012	IHC-P	1:250	
Goat anti-Rabbit IgG HRP	Anti-Rabbit IgG, HRP-linked Antibody	Cell Signaling Technology	7074	Western Blot	1:2000	
HA	Anti-HA-Peroxidase	Roche	12013819001	Western Blot	1:500	
ITGB4	Anti-ITGB4 antibody	Sigma-Aldrich	HPA036348	IHC-P	1:100	HIER: Tris-EDTA pH 10
IVL	Anti-involucrin Antibody (A-5)	Santa Cruz Biotechnology	sc-398952	IHC-P	1:100	HIER: either 10 mM Sodium Citrate pH 6 or Tris-EDTA pH 10
KRT1	Cytokeratin 1 (human) monoclonal antibody (34βB4)	Enzo Life Sciences	C34904	IHC-P (TMA)	-	
PCNA	Anti-PCNA Antibody (PC10)	Santa Cruz Biotechnology	sc-56	IHC-P	1:100	HIER: Tris-EDTA pH 10
PTPN14	PTPN14 (D5T6Y)	Cell Signaling Technology	13808	Western Blot	1:500	
TAZ	TAZ (D3I6D)	Cell Signaling Technology	70148	Western Blot	1:1000	
V5	Anti-V5 Tag Antibody	Invitrogen	46-0705	Western Blot	1:1000	
YAP1	YAP (D8H1X) XP	Cell Signaling Technology	14074	IHC-P	1:50	HIER: Tris-EDTA pH 10
YAP1	YAP (D8H1X) XP	Cell Signaling Technology	14074	Western Blot	1:1000	

Supplemental File 2
Organotypic cultures used in the study

Homogenous HFK Organotypic Cultures

Raft Condition	White Lab ID	Vector	HFK Donor	List of Figures *inclusion of a single culture in >1 figure indicates that separate sections of the culture were processed independently					
HFK-1	0807201032 HFK	None	4659	Figure 2B	Figure 1-figure supplement 3C	Figure 2-figure supplement 2A			
HFK-2	0609211130 HFK 1	None	4659	Figure 1E	Figure 1-figure supplement 2A	Figure 1-figure supplement 2B	Figure 1-figure supplement 3A		
HFK-3	0609211130 HFK 2	None	4659	Figure 1B	Figure 1C	Figure 1D	Figure 3C	Figure 1-figure supplement 3B	Figure 1-figure supplement 4A
HPV18 LoxP-1	012720201431 WT 1	pNeo-loxP-HPV18	4659	Figure 1B	Figure 1C	Figure 1-figure supplement 2B			
HPV18 LoxP-2	012720201431 WT 2	pNeo-loxP-HPV18	4659	Figure 1-figure supplement 2A					
HPV16 E7 WT-1	040520211003 16E7-1	MSCV-P C-FlagHA 16E7	4659	Figure 1-figure supplement 2A	Figure 1-figure supplement 3B				
HPV16 E7 WT-2	040520211003 16E7-2	MSCV-P C-FlagHA 16E7	4659	Figure 1D	Figure 1E				
HPV18 E7 WT-1	072220201051 18E7 WT1	MSCV-P C-FlagHA 18E7	4659	Figure 1D	Figure 1-figure supplement 3A	Figure 1-figure supplement 4A			
HPV18 E7 WT-2	072220201051 18E7 WT2	MSCV-P C-FlagHA 18E7	4659	Figure 1-figure supplement 3C	Figure 2-figure supplement 2A				
HPV18 E7 WT-3	080720201032 18E7 WT1	MSCV-P C-FlagHA 18E7	4659	Figure 2B					
HPV18 E7 WT-4	080720201032 18E7 WT2	MSCV-P C-FlagHA 18E7	4659						
HPV18 E7 WT-5	080720201032 18E7 WT3	MSCV-P C-FlagHA 18E7	4659	Figure 2-figure supplement 2A					
HPV18 E7 R84S-1	072220201051 18E7 R84S1	MSCV-P C-FlagHA 18E7 R84S	4659						
HPV18 E7 R84S-2	072220201051 18E7 R84S2	MSCV-P C-FlagHA 18E7 R84S	4659	Figure 2-figure supplement 2A					
HPV18 E7 R84S-3	080720201032 18E7 R84S1	MSCV-P C-FlagHA 18E7 R84S	4659	Figure 2B					
HPV18 E7 R84S-4	080720201032 18E7 R84S2	MSCV-P C-FlagHA 18E7 R84S	4659	Figure 2-figure supplement 2A					
HPV16 E6-1	040520211003 16E6-2	MSCV-IP N-FlagHA 16E6	4659	Figure 1E					
HPV16 E6-2	040520211003 16E6-3	MSCV-IP N-FlagHA 16E6	4659	Figure 1-figure supplement 4A					

Homogenous N/Tert-Cas9 Organotypic Cultures

Raft Condition	White Lab ID	sgRNA	Cell Line	List of Figures *inclusion of a single culture in >1 figure indicates that separate sections of the culture were processed independently	
N/Tert-Cas9 Mock-1	072220201051 Mock1 N-Tert	None	N/Tert-Cas9	Figure 2A	Figure 2-figure supplement 1B
N/Tert-Cas9 Mock-2	072220201051 Mock2 N-Tert	None	N/Tert-Cas9	Figure 2-figure supplement 1A	Figure 2-figure supplement 1C
N/Tert-Cas9 sgPTPN14-1	072220201051 sgPTPN141 N-Tert	sgPTPN14-1	N/Tert-Cas9	Figure 2-figure supplement 1A	
N/Tert-Cas9 sgPTPN14-2	072220201051 sgPTPN142 N-Tert	sgPTPN14-1	N/Tert-Cas9	Figure 2-figure supplement 1B	
N/Tert-Cas9 sgPTPN14-3	072220201051 sgPTPN143 N-Tert	sgPTPN14-1	N/Tert-Cas9	Figure 2B	Figure 2-figure supplement 1C

Cell Fate Organotypic Cultures

Tracer Cell Condition	White Lab ID	Vectors in Tracer Cells	HFK Donor	Dilution (Tracer:Unmodified)	List of Figures
pLIX YAP1 WT (-)-1	082020211055 WT(-)1	pLIX YAP1 WT; pLenti CMV GFP Hygro (656-4)	4948	1:25	Figure 7A
pLIX YAP1 WT (-)-2	082020211055 WT(-)2	pLIX YAP1 WT; pLenti CMV GFP Hygro (656-4)	4948	1:25	
pLIX YAP1 WT (Dox)-1	082020211055 WT DOX 1	pLIX YAP1 WT; pLenti CMV GFP Hygro (656-4)	4948	1:25	Figure 7A
pLIX YAP1 WT (Dox)-2	082020211055 WT DOX 2	pLIX YAP1 WT; pLenti CMV GFP Hygro (656-4)	4948	1:25	
pLIX YAP1 S127A (-)-1	043020211353 CF S127A - 2	pLIX YAP1 S127A; pLenti CMV GFP Hygro (656-4)	4659	1:25	
pLIX YAP1 S127A (-)-2	082020211055 S127A(-)1	pLIX YAP1 S127A; pLenti CMV GFP Hygro (656-4)	4948	1:25	
pLIX YAP1 S127A (Dox)-1	043020211353 CF S127A DOX 1	pLIX YAP1 S127A; pLenti CMV GFP Hygro (656-4)	4659	1:25	
pLIX YAP1 S127A (Dox)-2	043020211353 CF S127A DOX 2	pLIX YAP1 S127A; pLenti CMV GFP Hygro (656-4)	4659	1:25	
pLIX YAP1 S127A (Dox)-3	082020211055 S127A DOX 1	pLIX YAP1 S127A; pLenti CMV GFP Hygro (656-4)	4948	1:25	
pLIX YAP1 S127A (Dox)-4	082020211055 S127A DOX 2	pLIX YAP1 S127A; pLenti CMV GFP Hygro (656-4)	4948	1:25	Figure 7A
pLIX YAP1 S94A (-)-1	082020211055 S94A(-)1	pLIX YAP1 S94A; pLenti CMV GFP Hygro (656-4)	4948	1:25	
pLIX YAP1 S94A (Dox)-1	082020211055 S94A DOX 1	pLIX YAP1 S94A; pLenti CMV GFP Hygro (656-4)	4948	1:25	Figure 7A
pLIX YAP1 S94A (Dox)-2	082020211055 S94A DOX 2	pLIX YAP1 S94A; pLenti CMV GFP Hygro (656-4)	4948	1:25	
LentiCRISPR sgNT-1-1	043020211353 CF sgNT-1 2	LentiCRISPR v2 sgNT-1; pLenti CMV GFP Hygro (656-4)	4659	1:25	
LentiCRISPR sgNT-1-2	10062021327 sgNT-1-1	LentiCRISPR v2 sgNT-1; MSCV GFP Neo C-HA	4952	1:25	
LentiCRISPR sgNT-1-3	10062211327 sgNT-1-2	LentiCRISPR v2 sgNT-1; MSCV GFP Neo C-HA	4952	1:25	
LentiCRISPR sgPTPN14-3-1	043020211353 CF sgPTPN14-3 1	LentiCRISPR v2 sgPTPN14-3; pLenti CMV GFP Hygro (656-4)	4659	1:25	
LentiCRISPR sgPTPN14-3-2	043020211353 CF sgPTPN14-3 2	LentiCRISPR v2 sgPTPN14-3; pLenti CMV GFP Hygro (656-4)	4659	1:25	
LentiCRISPR sgPTPN14-3-3	100620211327 sgPTPN14-3-1	LentiCRISPR v2 sgPTPN14-3; MSCV GFP Neo C-HA	4952	1:25	
LentiCRISPR sgPTPN14-3-4	10062021327 sgPTPN14-3-2	LentiCRISPR v2 sgPTPN14-3; MSCV GFP Neo C-HA	4952	1:25	
LentiCRISPR sgPTPN14-4-1	043020211353 CF sgPTPN14-4 1	LentiCRISPR v2 sgPTPN14-4; pLenti CMV GFP Hygro (656-4)	4659	1:25	
LentiCRISPR sgPTPN14-4-2	043020211353 CF sgPTPN14-4 2	LentiCRISPR v2 sgPTPN14-4; pLenti CMV GFP Hygro (656-4)	4659	1:25	
LentiCRISPR sgPTPN14-4-3	10062211327 sgPTPN14-4-1	LentiCRISPR v2 sgPTPN14-4; MSCV GFP Neo C-HA	4952	1:25	
LentiCRISPR sgPTPN14-4-4	100620211327 sgPTPN14-4-2	LentiCRISPR v2 sgPTPN14-4; MSCV GFP Neo C-HA	4952	1:25	
Empty Vector-1	102620201147 Empty	MSCV-Neo C-HA Empty; PHAGE-P-CMVt N-HA GFP	4659	1:50	
Empty Vector-2	90220211137 48 EV 1	MSCV-Neo C-HA Empty; PHAGE-P-CMVt N-HA GFP	4948	1:50	Figure 7-figure supplement 2A
Empty Vector-3	90220211137 48 EV 2	MSCV-Neo C-HA Empty; PHAGE-P-CMVt N-HA GFP	4948	1:50	Figure 7C
Empty Vector-4	90220211137 52 EV 1	MSCV-Neo C-HA Empty; PHAGE-P-CMVt N-HA GFP	4952	1:50	
Empty Vector-5	90220211137 52 EV 2	MSCV-Neo C-HA Empty; PHAGE-P-CMVt N-HA GFP	4952	1:50	
HPV18 E7 WT-1	102620201147 18E7	MSCV-Neo C-HA 18E7; PHAGE-P-CMVt N-HA GFP	4659	1:50	
HPV18 E7 WT-2	90220211137 48 WT 1	MSCV-Neo C-HA 18E7; PHAGE-P-CMVt N-HA GFP	4948	1:50	Figure 7C
HPV18 E7 WT-3	90220211137 48 WT 2	MSCV-Neo C-HA 18E7; PHAGE-P-CMVt N-HA GFP	4948	1:50	
HPV18 E7 R84S-1	102620201147 R84S	MSCV-Neo C-HA 18E7 R84S; PHAGE-P-CMVt N-HA GFP	4659	1:50	
HPV18 E7 R84S-2	90220211137 48 R84S 1	MSCV-Neo C-HA 18E7 R84S; PHAGE-P-CMVt N-HA GFP	4948	1:50	
HPV18 E7 R84S-3	90220211137 48 R84S 2	MSCV-Neo C-HA 18E7 R84S; PHAGE-P-CMVt N-HA GFP	4948	1:50	Figure 7C
HPV18 E7 ΔDLLC-1	90220211137 48 dDLLC 1	MSCV-Neo C-HA 18E7 ΔDLLC; PHAGE-P-CMVt N-HA GFP	4948	1:50	Figure 7-figure supplement 2A
HPV18 E7 ΔDLLC-2	90220211137 52 dDLLC 1	MSCV-Neo C-HA 18E7 ΔDLLC; PHAGE-P-CMVt N-HA GFP	4952	1:50	

Supplemental File 3

Tumor microarray specimen information

	Oral Cavity	Oropharynx	Total	HPV-positive	HPV-negative*
# Patients	72	48	120	33	87
Primary tumor (T-stage) †					
Early (T1 or T2)	60	40	100	27	73
Advanced (T3 or T4)	12	8	20	6	14
Nodal metastasis					
Positive	24	39	63	29	34
Negative	48	9	57	4	53
Overall pathologic stage †					
Early (I or II)	43	7	50	3	47
Advanced (III or IV)	29	41	70	30	40

*HPV status was defined by IHC for p16 for oropharyngeal tumors during routine clinical and was inferred as negative for oral cavity tumors per standards of the College of American Pathologists (Lewis et al. (2018) Archives of Pathology & Laboratory Medicine 142:559–597).

† 7th edition AJCC staging manual

Supplemental File 4

Gene Lists for Pathway Mutational Analyses

HIPPO Pathway	Cell Cycle	p53
STK4	CDKN1A	TP53
STK3	CDKN1B	MDM2
SAV1	CDKN2A	MDM4
LATS1	CDKN2B	ATM
LATS2	CDKN2C	CHEK2
MOB1A	CCND1	RPS6KA3
MOB1B	CCND2	
YAP1	CCND3	
WWTR1	CCNE1	
TEAD1	CDK2	
TEAD2	CDK4	
TEAD3	CDK6	
TEAD4	RB1	
PTPN14	E2F1	
NF2	E2F3	
WWC1		
TAOK1		
TAOK2		
TAOK3		
CRB1		
CRB2		
CRB3		
LLGL1		
LLGL2		
HMCN1		
SCRIB		
HIPK2		
FAT1		
FAT2		
FAT3		
FAT4		
DCHS1		
DCHS2		
CSNK1E		
CSNK1D		
AJUBA		
LIMD1		
WTIP		